Environmental Modelling and Software 111 (2019) 134–152

Contents lists available at ScienceDirect

Environmental Modelling & Software

journal homepage: www.elsevier.com/locate/envsoft

A toolbox for the optimal design of run-of-river hydropower plants

Veysel Yildiz[a], Jasper A. Vrugt[a,b,*]

[a] Department of Civil and Environmental Engineering, University of California Irvine, 4130 Engineering Gateway, Irvine, CA, 92697-2175, United States
[b] Department of Earth System Science, University of California Irvine, Irvine, CA, United States

ARTICLE INFO

Keywords:
Run-of-river (RoR) hydropower plant
Impulse and reaction turbines
Differential evolution (DE)
Net present value (NPV)
Capital and investment costs
Flow duration curve (FDC)

ABSTRACT

Hydroelectric power is a relatively cheap, reliable, sustainable, and renewable source of energy that can be generated without toxic waste and considerably lower emissions of greenhouse gases than fossil fuel energy plants. Conventional hydroelectric plants produce energy by the controlled release of dammed reservoir water to one or more turbines via a penstock. The kinetic energy of the falling water produces a rotational motion of the turbine shaft and this mechanical energy is converted into electricity via a power generator. Dam-based plants are among the largest and most flexible power producing facilities in the world, yet their construction and operation is costly and can damage and disrupt upstream and downstream ecosystems and have catastrophic effects on downriver settlements and infrastructure. Run-of-the-river (RoR) hydroelectric stations are an attractive and environmentally friendly alternative to dam-based facilities. These plants divert water from a flowing river to a turbine and do not require the formation of a reservoir. Despite their minimal impact on the surrounding environment and communities, the potential of RoR plants has not been fully explored and exploited. For example, in the United States it is estimated that RoR plants could annually produce 60, 000 MW, or about 13% of the total electricity consumption in 2016. Here, we introduce a numerical model, called HYdroPowER or HYPER, which uses a daily time step to simulate the technical performance, energy production, maintenance and operational costs, and economic profit of a RoR plant in response to a suite of different design and construction variables and record of river flows. The model is coded in MATLAB and includes a built-in evolutionary algorithm that enables the user to maximize the RoR plant's power production or net economic profit by optimizing (among others) the penstock diameter, and the type (Kaplan, Francis, Pelton and Crossflow) design flow, and configuration (single/parallel) of the turbine system. Unlike other published models, this module of HYPER carefully considers each turbine's design flow, admissible suction head, specific and rotational speed in evaluating the technical performance, cost and economic profit of a RoR plant. Two case studies illustrate the power and practical applicability of HYPER. Some of their results confirm earlier literature findings, that (I) the optimum capacity and design flow of a RoR plant is controlled by the river's flow duration curve, (II) a highly variable turbine inflow compromises energy production, and (III) a side-by-side dual turbine system enhances considerably the range of workable flows, operational flexibility and energy production of a RoR plant. HYPER includes a GUI and is available upon request from the authors.

1. Introduction and scope

Throughout history, human population growth has been supported by a steadily increasing production and consumption of energy. In the most recent four decades, the per capita energy consumption has increased from a global average of 1.56 tonnes of oil equivalent (toe) per person in 1973 to 1.66 toe per person in 2000 and 1.92 toe per person in 2014 (The World Bank, 2017). This ever increasing demand for energy poses important challenges as the continued reliance on conventional (nonrenewable) sources such as coal, natural gas and petroleum (fossil fuels) has profoundly negative health, environmental and climatic impacts. For example, the extraction of fossil fuels by strip mining and mountaintop removal of coal degrades the environment and damages ecological systems (Palmer et al., 2010). Their combustion for electricity generation by power stations leads to greenhouse gas emissions, atmospheric pollution by nitrogen oxides, soot, volatile organic compounds, many other (fine) particulates, and smog with high levels of ozone. These emissions, in particular the large amounts of released carbon dioxide, are the main cause of global warming according to the Intergovernmental Panel on Climate Change (IPCC).

* Corresponding author. Department of Civil and Environmental Engineering, University of California Irvine, 4130 Engineering Gateway, Irvine, CA, 92697-2175, United States.
E-mail address: jasper@uci.edu (J.A. Vrugt).

https://doi.org/10.1016/j.envsoft.2018.08.018
Received 2 August 2017; Received in revised form 18 August 2018; Accepted 22 August 2018
Available online 28 August 2018
1364-8152/

Renewable energy sources such as wind, solar, geothermal, biomass and hydropower are a more clean, sustainable, and environmentally friendly alternative to traditional, nonrenewable, energy sources. These so-called *green* energy sources are replenished naturally on human timescales and reduce environmental pollution and global warming emissions. In 2015, renewable energy comprised about 10% of the energy consumption in the United States, of which 49% originates from biomass (biofuels, wood, waste), 8% is made up of heat energy (geothermal and solar), 19% signifies electricity from wind, and 25% constitutes hydroelectric power (US Energy Information Administration, 2016). Of these, hydropower is one of the least expensive renewable energy sources with a price competitive to fossil fuels, gas, and biomass. Indeed, hydropower is the only regenerative energy source to supply electricity on an industrial scale at competitive prices (Delucchi and Jacobson, 2011; Berga, 2016). Yet, less than one third of the hydroelectric potential on our planet is currently exploited (Basso and Botter, 2012).

Hydroelectric power is a relatively cheap, reliable, sustainable, and renewable source of energy that can be generated without toxic waste and considerably lower emissions of greenhouse gases than fossil fuel energy plants (Dursun and Gokcol, 2011; Demarty and Bastien, 2011; Mao et al., 2017). Conventional hydroelectric plants produce energy by the controlled release of dammed reservoir water to one or more turbines via a penstock. The kinetic energy of the falling water produces a rotational motion of the turbine shaft and this mechanical energy is converted into electricity via a power generator. In 2010, the world commission of dams has estimated the potential production of hydroelectric energy to be more than four times the current annual worldwide generation (IJHD, 2010). Currently, hydropower plants produce about 20% of all electricity used world-wide (10% in United States) and this percentage is expected to increase substantially in the coming years as the world is slowly moving away from fossil fuels in lieu of more sustainable and environmentally friendly sources of energy. More than 60 countries in the world derive at least half of their entire electricity production (demand) from hydropower plants (GVR, 2014; Lafitte, 2014).

Dam-based plants are among the largest and most flexible power producing facilities in the world, yet their construction and operation is costly, can damage and disrupt upstream and downstream ecosystems and have catastrophic effects on downriver settlements and infrastructure. Legislation in many countries therefore prohibits further construction of such plants (Paish, 2002a,b). Small hydropower stations are a viable, clean and cost-effective alternative to dam-based plants, and provide the option of decentralized power production. Such plants not only simplify rural electrification in less-developed countries, but also hold great promise for continents such as Europe which has exhausted large-scale hydropower production, and is seeking better and less invasive ways of energy production. Small hydro-electric plants require a relatively large initial investment (construction cost), yet their relatively low operation and maintenance costs, long-life span and negligible socioeconomic impacts are highly desirable (Kumar et al., 2011) and have propelled small hydropower stations to the center stage of the energy debate (Okot, 2013). Note, that it is not always easy to classify hydroelectric plants as small or large, in part because of contrasting developmental policies and large differences in size and population of countries (Paish, 2002a; Egré and Milewski, 2002; Kumar et al., 2011). Nevertheless, most operational hydro plants in the world today are considered small and have a maximum production capacity of 15 MW per year.

The vast majority of small hydroelectric stations in the world are so called run-of-the-river (RoR) plants. These plants can be installed at existing dams, as independent generating facilities, or in private systems that power small communities, and use a channel or penstock to divert water from the river stream (up to 95% of mean annual discharge) to one or more turbines with electric generators (Douglas, 2007; Knight Piesold Consulting, 2008). The diverted river water will rotate the turbine shaft, and the resulting mechanical energy is converted into electricity by the generator. Downstream the diverted water is released back to the river. Thus, RoR plants produce hydro-electrical energy without use of a large water storage reservoir. This equates to a relatively low installed capacity of 1–50 Mega Watt (MW). Exceptions include the Chief Joseph Dam in the United States with installed capacity of about 2620 MW.

RoR plants have a much smaller impact on the local ecosystem than their dammed counterparts, and their construction is shorter and less complex requiring an overall lower capital investment (Abbasi and Abbasi, 2011; Okot, 2013). Furthermore, these plants are better amenable to smaller water heads, and offer the possibility of decentralized electrification at relatively low operational and maintenance costs. Yet, their lack of a major reservoir has an important side-effect, and that is, that their power production is not constant but dependent on natural variations in river discharge. Electricity production may even cease when water levels in the river drop because of droughts or water extraction, and the discharge drops below the minimum technical inflow of the turbines. Note, that most RoR stations are equipped with a small dam or weir to satisfy base load demands during wet seasons and manage peak load demands during dry seasons (wivedi and Raja, 2006).

During the past three decades much research has been devoted to the optimal design, operation and performance of RoR hydropower plants. That research has focused primarily on five different issues: (1) the determination of the optimum RoR plant capacity, (2) the development of specialized metrics (indexes) that convey properly the economic performance (profitability) and energy production of RoR power plants, (3) the development of efficient optimization approaches that can solve rapidly for the optimal RoR design, (4) the design, operation, analysis, and performance of turbines, and (5) the importance of streamflow processes and surface hydrology on the overall performance of the RoR plant.

Research into the optimum size (capacity) of RoR plants (1) has focused primarily on maximization of investment profitability and/or economic return (Sharma et al., 1980, 2002; Gingold, 1981; Fahlbuch, 1983, 1986; Deppo et al., 1984; Najmaii and Movaghar, 1992; Voros et al., 2000; Montanari, 2003; Hosseini et al., 2005; Anagnostopoulos and Papantonis, 2007; Haddad et al., 2011; Santolin et al., 2011; Basso and Botter, 2012). General consensus is that it is particularly difficult to define an optimum size of the turbines of a RoR plant, in large part because of the rather unrealistic assumption of constant turbine inflows. Furthermore, Mishra et al. (2011) concluded that the properties of the river discharge and number of poles of the generator determine the optimum size and investment costs of small hydropower plants, nevertheless, these variables are often ignored during design, installation and optimization analysis. Moreover, the optimum size of the turbines depends strongly on the characteristics of the installation site, actual turbines used, and the main performance metric of the RoR plant (Fahlbuch, 1983; Deppo et al., 1984; Papantonis and Andriotis, 1993; Voros et al., 2000; Kaldellis et al., 2005; Hosseini et al., 2005). Detailed numerical simulation is required to estimate the maximum capacity of a RoR plant for given site characteristics and record of discharge observations (Lopes de Almeida et al., 2006; Anagnostopoulos and Papantonis, 2007; Papantonis and Andriotis, 1993; Haddad et al., 2011).

Research into performance measures of RoR power plants (2) has led to the development of several specialized metrics. These metrics can be grouped into three main categories including variables that measure the economic performance (Voros et al., 2000; Hosseini et al., 2005; Motwani et al., 2013; Nouni et al., 2006), operational efficiency (Liu et al., 2003), and power production (Karlis and Papadopoulos, 2000; Aslan et al., 2008; Niadas and Mentzelopoulos, 2008). Economic indices include criteria such as the net present value (Deppo et al., 1984; Brealey and Myers, 2002; Karlis and Papadopoulos, 2000; Hosseini et al., 2005; Kaldellis et al., 2005; Nouni et al., 2006; Anagnostopoulos

and Papantonis, 2007; Santolin et al., 2011; Basso and Botter, 2012), efficiency maintenance, operational maintenance (Liu et al., 2003), internal rate of return (Karlis and Papadopoulos, 2000; Kaldellis et al., 2005; Santolin et al., 2011; Basso and Botter, 2012; Kaldellis et al., 2005, 2005), pay-back time (Karlis and Papadopoulos, 2000) and benefit-cost ratio (Hosseini et al., 2005; Karlis and Papadopoulos, 2000; Nouni et al., 2006; Anagnostopoulos and Papantonis, 2007). The operational efficiency of the RoR plant can be defined using metrics such as the overall efficiency, ideal efficiency, and reachable efficiency (Liu et al., 2003). The power production is simply equivalent to the total mechanical energy produced by the RoR plant. Of all these metrics, the net present value and the annual power production are used most commonly in the hydropower literature to evaluate the performance of RoR hydroelectric plants.

Research into optimization algorithms (3) has led to the development and use of linear, nonlinear and quadratic programming, hybrid mixed-integer variants, interior point methods, (quasi)-Newton method, and more flexible stochastic and evolutionary optimization algorithms (Deppo et al., 1984; Najmaii and Movaghar, 1992; Montanari, 2003; Hosseini et al., 2005; Fleten and Kristoffersen, 2008; Finardi et al., 2005; Lopes de Almeida et al., 2006; Anagnostopoulos and Papantonis, 2007; Yoo, 2009; Haddad et al., 2011; Baños et al., 2011; Basso and Botter, 2012). The application of optimization techniques to power system planning and operation has been an area of active research since the early 1960s. Many different approaches have been developed for tracing the flow of electric power in a network (Momoh et al., 1999a; b). Some of these methods have found application for backing out the optimal design and management of RoR plants. We refer to Baños et al. (2011) for a comprehensive review of optimization algorithms for design, planning and control of hydropower plants. Altogether, published findings demonstrate that evolutionary algorithms are preferred over more simplistic analytic approaches and/or linear/nonlinear/quadratic programming methods, because of their ease of implementation and use, and ability to handle efficiently many different decision variables. Of these, genetic algorithms have found widespread use in the water resources planning and management literature (Nicklow et al., 2010). Maier et al. (2014) summarizes the current status, research challenges and future directions of evolutionary algorithms and other metaheuristics in water resources applications.

Research into turbine selection, design, analysis, operation and performance (4) has led to approaches for direct measurement, monitoring, numerical simulation, and optimization of the turbine efficiency (Gibson, 1923; Troskolanski, 1960; IEC, 1991; Khosrowpanah et al., 1988; Desai and Aziz, 1994; Williams, 1994; Ye et al., 1995; Parker, 1996; Zheng, 1997; Olgun, 1998; Ye et al., 2000; Liu, 2000; Adamkowski et al., 2006; Ye-xiang et al., 2007; Wallace and Whittington, 2008; Derakhshan and Nourbakhs, 2008; Singh and Nestmann, 2009; Alexander et al., 2009; Yassi and Hashemloo, 2010; Akinori et al., 2010; Anagnostopoulos and Dimitris, 2012; Shimokawa et al., 2012; Ramos et al., 2013; Bozorgi et al., 2013; Khurana et al., 2013; Williamson et al., 2013; Laghari et al., 2013; Pimnapat et al., 2013; Cobb and Sharp, 2013; Williamson et al., 2014; Yaakob et al., 2014; Elbatran et al., 2015) The pressure-time method (Gibson, 1923; Troskolanski, 1960; IEC, 1991; Adamkowski et al., 2006) is one of the few methods available to measure accurately the absolute water flow rate, a key variable that determines the turbine efficiency. This requires installation of several pressure sensors at selected sections of the turbine penstock. This task is expensive when the penstock is not exposed. The excellent review of Elbatran et al. (2015) provides an in-depth summary of the performance, operation cost of low head, hydropower turbines. Other turbines have been discussed at length in the cited publications. In general, the cited literature above has demonstrated that numerical modeling, experimental investigations, and multi-criteria decision analysis are key to determining an appropriate turbine for given site characteristics and flow values. Moreover, the use of two or more turbines of different size (and or type) improves considerably the ability of a RoR plant to respond effectively to seasonal variations in the discharge (Anagnostopoulos and Papantonis, 2007).

Finally, research into the influence of streamflow hydrology on operation of RoR plants (5) has led to spreadsheet software and flexible parametric expressions or probabilistic/stochastic approximations of the flow duration curve (FDC) that can be used to evaluate design and economic performance (Heitz, 1982; USACE, 1985; Vogel and Fennessey, 1995; Hobbs et al., 1996; Borges and Pinto, 2008; Singh and Nestmann, 2009; Niadas and Mentzelopoulos, 2008; Peña et al., 2009; Heitz and Khosrowpanah, 2012). Probabilistic approaches are preferred as they take account explicitly for uncertainties in the turbine inflows when designing RoR plants. The mathematical expressions of the FDC introduced by Sadegh et al. (2015) are particularly powerful for RoR plant evaluation when coupled with uncertainty quantification using Bayesian inference with DREAM (Vrugt et al., 2008, 2009).

Despite the shorter construction times, lower capital investment and desirable environmental advantages of RoR plants, their energy production is not constant but rather varies dynamically with river discharge originating from rainfall and/or snowpack melting. Indeed, turbine inflows may vary significantly between days and seasons depending on weather and prevailing climatic conditions of the river network (watershed). This complicates tremendously the design (e.g. penstock diameter, turbine type, number and configuration) and operational use (design flow) of RoR plants. For example, an investigation into the operation of hydropower plants in Malaysia has shown that a 1 percent improvement in the efficiency of the turbines could lead to a 1.25% increase in earnings (Al-Zubaidy and Right, 1997). Of course, some power loss is unavoidable during energy conversion, yet this loss can be minimized with a proper design.

Integrated environmental modeling (IEM) can help elucidate a suitable design and complexity of a RoR plant which maximizes energy production and net profit under a variable river discharge, hydrostatic head and kinetic energy of the flowing water. IEM provides a science-based approach to organize and integrate multidisciplinary knowledge in a modeling, simulation, and decision-making framework, and use this know-how to explain, explore, simulate, and forecast the response of complex environmental systems to natural and human-induced conditions. This approach can link computer models, economic analysis, management practice and planning, and control and systems theory to seek, explore, and test potential solutions to complex environmental problems. This necessitates knowledge transfer between domain experts in different fields of study (Parker et al., 2002; MEA, 2005; Letcher et al., 2006; Laniak et al., 2013; Hamilton et al., 2015), and the development of computer software and decision support frameworks which integrate domain-specific knowledge and data. Optimization methods (evolutionary algorithms) play a key role herein and their use is becoming increasingly more common in water management for policy, planning, and operational decision-making (Nicklow et al., 2010; Maier et al., 2014).

In this paper, we present an example of an integrated environmental modeling framework and describe the different building blocks (equations) of a generic numerical model of a RoR power plant. This model, called HYdroPowER, or HYPER, is coded in MATLAB, and uses a daily time step to simulate the technical performance, energy production, maintenance and operational costs, and economic profit of a RoR plant in response to a record of river flows and suite of different design and project variables.

HYPER differs in several important ways from existing RoR modeling approaches published in the hydropower literature (Deppo et al., 1984; Najmaii and Movaghar, 1992; Voros et al., 2000; Montanari, 2003; Hosseini et al., 2005; Anagnostopoulos and Papantonis, 2007; Haddad et al., 2011; Santolin et al., 2011; Basso and Botter, 2012). In the first place, HYPER uses the specific speed as guiding principle to determine the most appropriate turbine(s) for given site characteristics and record of river flows. Our implementation improves upon the work of Santolin et al. (2011) who assumed erroneously non-overlapping

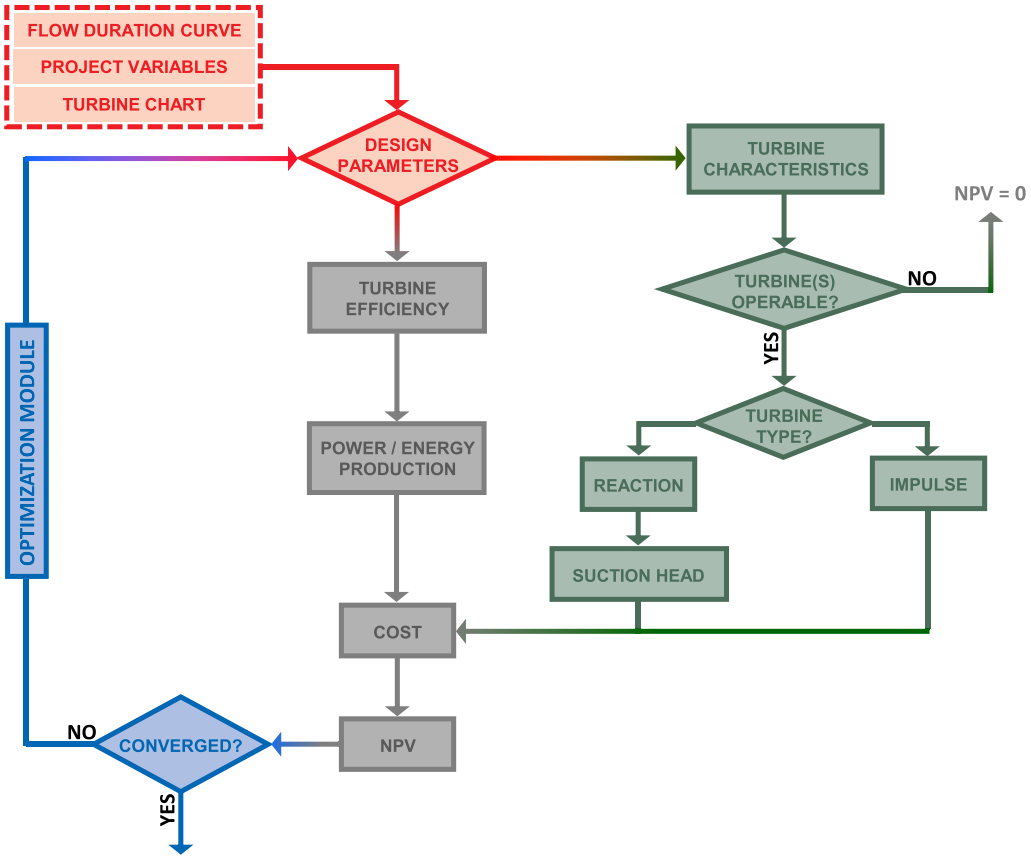

Fig. 1. High-level overview of HYPER with color coding for the different building blocks of the model. HYPER simulates the daily performance, investment, operation and maintenance costs, and economic profit of a RoR hydropower plant. Model inputs are highlighted in red. The design parameters (red diamond) play a key role in HYPER as they control the electricity production (gray), operational feasibility of the turbine system (green) and total costs (gray) of the RoR plant. A built-in optimization module (in blue) can be used to find optimal values of the design and/or project variables that maximize the net present value (NPV) of the plant. HYPER accommodates many other design objectives as well. (For interpretation of the references to color in this figure legend, the reader is referred to the Web version of this article.)

specific speeds of the different turbines. Secondly, HYPER simulates all relevant turbines (Kaplan, Pelton, Fancis and Crossflow) using input from the turbine chart of Penche (1998). The use of the Crossflow turbine addresses a critical deficiency in the hydropower literature as this turbine is commonly ignored in published studies due to its supposed inferior efficiency. Thirdly, HYPER accommodates single and dual (side-by-side or parallel) turbine systems. This advances upon the work of Anagnostopoulos and Papantonis (2007) who ignored inadvertently cavitation problems and the important role of the specific speed in turbine selection. HYPER contains a built-in optimization module which enables the user to maximize the RoR plants power production or net economic profit by optimizing (among others) design and project variables such as the penstock thickness, penstock diameter and the type (Kaplan, Francis, Pelton and Crossflow), quantity, design flow, and configuration (single or parallel) of turbines. This optimization module considers explicitly each turbine's design flow, suction head (for cavitation), and specific and rotational speed. This module is easy to execute and allows users to handpick and optimize relevant project and decision variables. Furthermore, HYPER includes a graphical user interface (GUI) to simplify model setup, numerical simulation, and selection and optimization of the decision variables. Finally, a post-processor generates graphical output which summarizes the daily performance of the RoR plant. The output of HYPER may serve as input to ecosystem models to evaluate the ecologic impacts of RoR plants.

The remainder of this paper is organized as follows. Section 2 introduces the main building blocks of HYPER. In this section we are especially concerned with the energy production of a RoR plant, and the technical characteristics of the turbines, turbine selection, operation and cavitation, characteristics of the four different types of turbines, their operation, and cavitation of the turbine blades. In section 3 we discuss the differential evolution global optimization algorithm that is used to optimize the main design variables of the RoR plant. This is followed in section 4 with two illustrative case studies which demonstrate the power and numerical results of HYPER. The penultimate section of this paper (section 5) introduces the GUI of HYPER. Finally, section 6 concludes this paper with a summary of our main findings.

2. Numerical model: equations, energy production and turbine specification

One of the main goals of the present study is the development of a numerical model that simulates accurately for given site characteristics the energy production and economic cost of a RoR hydro-electric plant in response to a suite of design and construction variables and a time series of river discharge (inflow) values. This simulator is the outcome of three formal stages to model building, including development of a

1 Conceptual model: Summarizes our abstract state of knowledge about the structure and workings of the RoR plant.
2 Mathematical model: Defines the computational states, fluxes, and parameters of the RoR plant and the choices regarding how system processes will be handled mathematically.
3 Computational model: Provides numerical solutions for specific site characteristics (head), design and operation parameters (decision variables), turbine selection and construction (penstock diameter and thickness), and boundary conditions (inflows)

We focus attention on the computational model of the RoR plant, and discuss in detail how the power production and economic costs of investment and maintenance depend on the selection of turbine type, site characteristics (net head, inflow) and the main project (e.g. Table 2) and design variables (e.g. size of penstock, turbine design flow). The model, coined HYdroPowER, or HYPER, is coded in MATLAB, and (a) uses the specific speed as guiding principle to determine the most appropriate turbine(s) for given site characteristics and record

of river discharge values, (b) simulates the Pelton, Francis, Kaplan and Crossflow turbines, and (c) accommodates single and dual, side-by-side turbine systems. In summary, HYPER constitutes the first numerical model that takes into explicit consideration the design flow, penstock diameter, penstock thickness, specific speed, rotational speed, and admissible suction head (to combat cavitation) in evaluating the technical performance, energy production, management and operational costs, and economic profit of a RoR plant. Moreover, a built-in evolutionary algorithm allows optimization of the design and project parameters, including turbine selection and configuration. This module is easy to execute and allows users to handpick and optimize relevant project and decision variables. HYPER includes a graphical user interface (GUI) to simplify model setup, numerical simulation, and selection and optimization of the decision variables. Finally, graphical output is produced by a post-processor which summarizes the daily performance of the RoR plant.

Fig. 1 presents a high-level overview of our modeling framework. Color coding is used to distinguish between the different building blocks of HYPER. Model inputs are highlighted in red and include the turbine chart, the flow duration curve, project variables (specified for later use in Table 2) and design parameters (discussed in detail in next section) of the installation site. The design parameters (in red diamond) not only govern the plant's electricity production and investment, operation and maintenance costs (grey track), but also control the technical characteristics (e.g. rotational speed and suction head) of the turbines. These characteristics must satisfy manufacturer guidelines, otherwise the turbine system is deficient and cannot operate. The design parameters and project variables can be specified by the user or their values can be determined via a built-in optimization module (in blue). This module implements an evolutionary search algorithm and allows users to maximize (or minimize, if appropriate) a suite of different design objectives. The present chart returns the net present value, or NPV, of the plant. This metric measures the net difference between all revenues received from the produced hydroelectric energy and the life time costs of the plant.

The remainder of this paper discusses in detail the different building blocks of our model and optimization framework. We start in the next section with the main equations of our model.

2.1. Energy production

The amount of energy, E, in kilowatt hours (kWh) a T-turbine hydropower plant ($T \geq 1$) can produce over a time period, Δt (days), can be calculated using

$$E(t) = \frac{24}{1000} \int_{t}^{t+\Delta t} \eta_g \rho_w g H_{net}\{q(t), D\} \sum_{j=1}^{T} [q_j(t) \eta_j\{q_j(t), O_{dj}\}] dt, \quad (1)$$

where t (days) denotes time, η_g $(-)$ is the generator efficiency, ρ_w (kg/m^3) is the density of water, g (m/s^2) signifies the gravitational constant, H_{net} (m) is the net head or water pressure at the bottom of the penstock, q (m^3/s) represents the inflow to the turbine system, D (m) denotes the penstock diameter, and q_j (m^3/s), O_{dj} (m^3/s) and η_j $(-)$ characterize the volumetric water flux, design flow and efficiency of the jth turbine, respectively. The curly braces make evident that the values of H_{net} and η_j are time dependent and vary as function of turbine inflow, penstock diameter and/or design flow, respectively. The multiplication factor in front of the integral sign converts the units of E from Watts day to kWh. The installed capacity of the hydropower plant, P, in megawatt (MW) can now be calculated using

$$P = \frac{1}{10^6} \eta_g \rho_w g H_{net} \left\{ \sum_{j=1}^{T} O_{dj}, D \right\} \sum_{j=1}^{T} O_{dj} \eta_j, \quad (2)$$

where the multiplication factor in front converts the units of P from Watt to MW.

The variables in Equation (1) elucidate that the power production depends on the local characteristics of the installation site, H_{net}, the turbine inflows, and turbine and generator efficiencies. Turbine efficiency is determined by the ratio of the volume flux of water it receives per time unit, q_j (inflow), and its design flow, O_d, hence $\eta_j \sim q_j(t)/O_{dj}$. In the next section we will discuss in detail the characteristics of commonly used turbines, and depict their efficiency curves. Note that the turbine inflow and net head have a linear effect on production.

Equation (1) cannot be solved analytically for dynamically varying boundary conditions and we therefore resort to numerical integration. A n-vector of mean daily turbine inflows, $\mathbf{q} = \{q(1), ..., q(n)\}$, is used to solve Equation (1) with a fixed daily integration time step. This vector of inflows is derived from observations of the hydrograph of the river network, $\mathbf{q}_r = \{q_r(1), ..., q_r(n)\}$. If such discharge measurements are not readily available then streamflow records from nearby catchments can be used, or alternatively a synthetic hydrograph can be defined. In the illustrative case studies presented herein we specify the n values of the discharge record by sampling from the FDC of the river network. This function depicts graphically the relationship between the exceedance probability of streamflow and its magnitude. Not all the streamflow that is transported by a river network can be diverted to the RoR plant. A fixed quantity of discharge, also called the minimum environmental flow, should be transported by the river network at all times to minimize adverse affects on the biotic environment within the stream. We therefore calculate the turbine inflow as follows

$$q(t) = \max(q_r(t) - q_{md}, 0), \quad (3)$$

where $q_r(t)$ (m^3/s) signifies the river discharge at time t, and q_{md} (m^3/s) is the minimum river discharge, or so-called minimum environmental flow, required to sustain ecosystem health. For simplicity, we assume a constant value of q_{md} in our numerical simulations with HYPER. If so desired, the program accommodates time-variable values of q_{md} (see e.g. Gorla and Perona (2013)).

The net head, H_{net} (m), varies as function of time and can be calculated as follows

$$H_{net}(t) = H_g - H_f(t) - H_o(t), \quad (4)$$

where H_g (m) denotes the gross head, H_f (m) represents the friction loss in the penstock, and H_o (m) measures the cumulative hydraulic losses in the conveyance system. The gross head, H_g, is equivalent to the difference in elevation of the upstream water level, z_{up}, and the downstream water level, z_{tail}, at the tail race

$$H_g = \begin{cases} z_{up} - z_{tail} & \text{reaction turbines} \\ z_{up} - z_{tail} - \delta_{jet} & \text{impulse turbines,} \end{cases} \quad (5)$$

where the gross head of impulse turbines must account for δ_{jet} (m), the height of the nozzle jet above the tail race. The gross head is constant and determined by plant design. The friction and hydraulic losses, H_f and H_o, respectively, depend upon river discharge, and consequently, are time-variant. The friction loss, H_f, is a function of the length, L (m), and diameter, D (m), of the penstock and can be calculated using the Darcy-Weisbach equation

$$H_f(t) = f \frac{L}{D} \frac{V(t)^2}{2g}, \quad (6)$$

where V (m/s) denotes the design velocity of the turbine inflow, f is a unitless friction factor, and g (m/s^2) signifies the gravitational acceleration. The flow velocity is simply calculated by dividing the inflow, $q(t)$, by the cross-sectional area of the penstock, A_p (m^2), or $V(t) = q(t)/A_p$. The singular losses, H_o, depend on the hydraulic geometry of the conveyance system and can be computed using

$$H_o(t) = k_{sum} \frac{V(t)^2}{2g}, \quad (7)$$

where k_{sum} $(-)$ is an aggregate resistance term that represents the

composite effect (summation) of screen, entrance, bend, and valve losses (Ramos et al., 2000).

The penstock conveys water from the river to the turbine system located at lower elevation, which converts into hydroelectricity the potential and kinetic energy of the flowing water. This enclosed pipe or tunnel is usually composed of a thin inner layer of steel encased by an outer shell of reinforced concrete to resist and withstand large internal water pressures. The penstock is equipped with a gate system to control the water inlet and may have grates or filters to trap debris. The penstock diameter, D, is one of the most important design parameters of a RoR hydropower plant. It not only determines the capacity and energy production of the hydropower system, but also governs the investment and maintenance costs of the plant. A small value of D is financially attractive but the penstock will suffer considerable friction (= head) losses (see Equation (6)). A large diameter penstock, on the contrary, can produce higher net heads, H_{net}, but at the expense of much larger investment and maintenance costs. This dichotomy can be expressed as follows

$$D_{\min} \leq D \leq D_{\max}, \tag{8}$$

where $D_{\min}$ and $D_{\max}$ signify the minimum and maximum allowable diameter of the penstock, respectively. Thus, the penstock diameter should be large enough to satisfy the design flow of the turbine system, yet cannot be too large, otherwise the penstock will be too expensive and too difficult to install (among others). Thus, the penstock diameter, D, is an important design parameter that warrants a detailed cost-benefit analysis of the RoR plant. We will further elaborate on this in a later section. The minimum thickness of the penstock, k (m), should satisfy

$$k = 0.0084D + 0.001, \tag{9}$$

so that the pipe can withstand the imposed water pressure.

2.2. Turbine selection: technical characteristics, operation and cavitation

The turbine system exerts a strong control on the energy production of a RoR hydroelectric plant as it converts the force of the diverted river water into electricity. Which turbine(s) to select depends in large part on site characteristics (e.g. available net head), and the river's discharge regime. In the past decades, a suite of different turbines have been developed to accommodate natural variations in head and discharge within and between river networks. Each of these turbines has a designated range of inflows. Outside this range the ability of the turbine to generate electrical power is significantly compromised.

In the present study, we investigate the performance of four commonly used turbines, namely Kaplan, Francis, Pelton and Crossflow. These turbines can be classified based on their physical principles of operation and, thus, how they convert into rotational motion the energy of the flowing water. The Pelton and Crossflow turbines are impulse turbines. In these two turbines, a nozzle directs a stream of high velocity water tangential to the turbine disc to which are affixed radial blades. The blades move in the direction of the water jet, with at least one blade always intercepting the stream. Energy is thus produced by water impinging on the blades of the runner.

The Francis and Kaplan turbines belong to the group of reaction turbines, and use the force exerted by the water to rotate the runner inside the turbine, in a way similar to how the engines of an airplane create trust. Reaction turbines exhibit a rather poor efficiency at low flows (see Fig. 2) despite their relatively high specific speeds. As these two turbines use profiled blades with special casings and guide vanes their operational use is more difficult than impulse turbines. Indeed, the blades of reaction turbines are costly, which make the Kaplan and Francis turbines rather expensive for operational use in RoR plants.

What sets impulse turbines apart from other turbines is that they exhibit a relatively high efficiency at low flows (see Fig. 2). In addition, they have a relatively simple design, which makes them easy to fabricate and maintain, and their performance is not much affected by sand and other dissolved particles. The Pelton and Crossflow turbines are therefore considered to be cost efficient for small RoR plants.

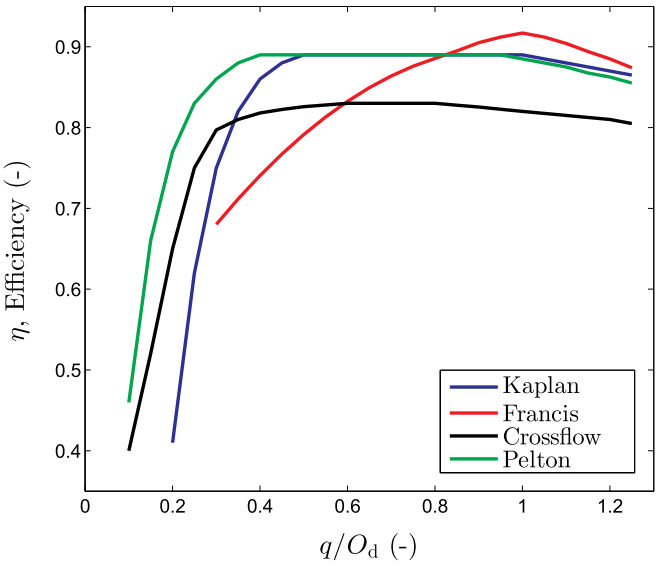

Fig. 2. Efficiency of the Kaplan (blue), Francis (red), Crossflow (black), and Pelton (green) turbines as function of the ratio between their flow rate and design flow respectively. (For interpretation of the references to color in this figure legend, the reader is referred to the Web version of this article.)

The efficiency, or characteristic, curve of a turbine determines in large part its suitability for a given installation site and river system. This curve can be obtained from the turbine manufacturer and depicts graphically the relationship between the ratio of the flow and design flow, q/O_{d} $(-)$, and the turbine efficiency, η $(-)$. This ratio is also referred to in the literature as design flow proportion, or percentage of full load (also called load). Efficiency curves are used in simulation studies to analyze how each turbine performs under specific conditions. Typical efficiency curves for the Kaplan, Francis, Pelton and Crossflow turbines are shown in Fig. 2. The following conclusions can be drawn from this turbine chart.

Impulse turbines (Crossflow and Pelton) exhibit a relatively high efficiency at loads smaller than 0.2 and a rather constant efficiency for loads between 0.25 and 1.2. The Pelton turbine (green) appears most promising with an efficiency that ranges from 0.80 to 0.89 for loads that vary between 0.2 and 1.2. The efficiency of the Crossflow turbine is consistently lower with about 10% for the plotted range of loads. Thus, impulse turbines possess a rather stable performance and remain relatively efficient for flows well below their design flow. Reaction turbines (Francis and Kaplan) can achieve a somewhat higher efficiency at full load, but their performance declines more rapidly towards lower loads. This is especially true for the Francis turbine whose efficiency deteriorates from values close to 0.93 at full load to values of about 0.7 at one-third of the design flow. For loads larger than 0.6, the Crossflow turbine exhibits the lowest efficiency. This may explain why this turbine is typically ignored in published studies in the hydropower literature. Nonetheless, impulse turbines (Crossflow and Pelton) have several desirable characteristics that promote their practical use in a RoR plant. Not only are they relatively inexpensive and easy to repair and maintain, they also exhibit a fairly constant efficiency for a large range of loads and are not susceptible to cavitation.

The net head and design flow determine the practical applicability of a turbine. The selection chart in Fig. 3 depicts schematically the operable range of net heads and design flows (inflows) of the Pelton (green), Crossflow (black), Kaplan (blue) and Francis (red) turbines simulated by HYPER. In general, impulse turbines (Crossflow and Pelton) can handle a large range of heads (3 - 1000 m) with low to

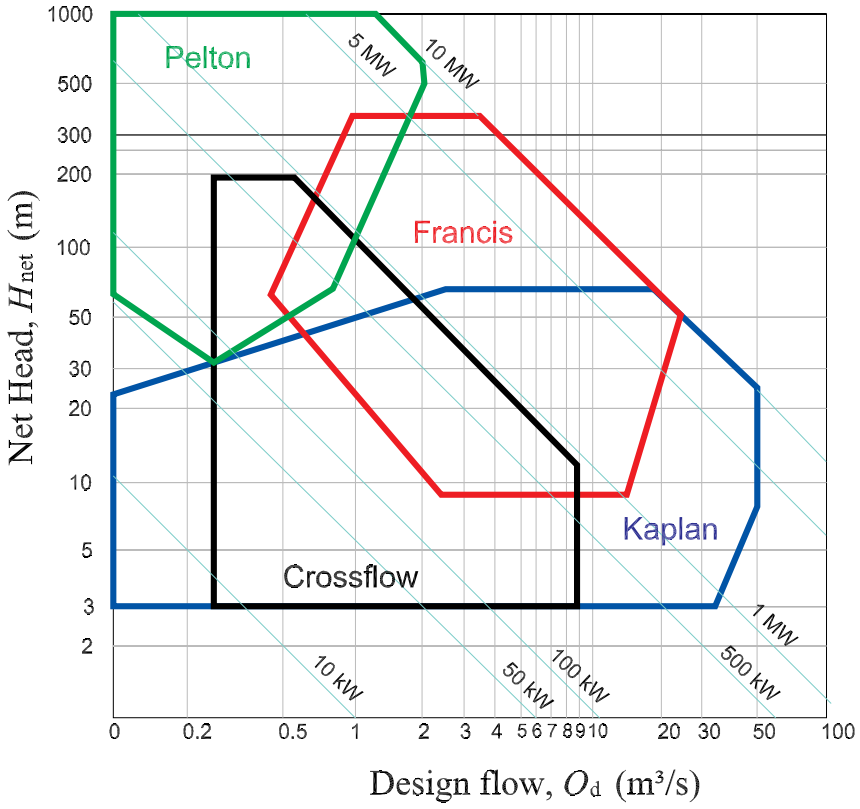

Fig. 3. Turbine chart (Penche, 1998).

medium design flows of 0–9 (m^3/s).

The Kaplan and Francis reaction turbines, on the contrary, cover a substantially smaller range of net heads of 3–70 m and 9–350 m, but with much enlarged design flows of 0–50 and 0.4–24 m^3/s, respectively. The selection chart makes evident that one can operate more than one turbine at a given design flow and net head. This complicates severely turbine selection. For example, the Crossflow, Francis and Pelton turbines all cover design flows of 0.75–1 m^3/s and net heads that vary between 50 and 170 m. Yet, this does not mean that each of these three turbines is equally good at producing hydroelectric energy within the specified ranges. This depends on the characteristic curves of the turbines (Fig. 2). What is more, turbines differ in their operation and maintenance costs. Indeed, this warrants an in-depth study of the performance of each turbine within HYPER. By comparing their annual energy production, investment, construction and maintenance costs, and economic profit, we can decide which turbine to select for given site characteristics and anticipated flow variability at the installation site. In general, the selection chart demonstrates that some turbines can handle a larger range of inflows than others and still operate at a relatively high efficiency.

The final choice which turbine(s) to select for a RoR plant involves an optimization analysis of expenditures (costs) versus benefits. Fig. 3 alone is thus insufficient to determine an appropriate turbine for a given installation site. Instead, the graph only dictates which turbines should be considered for a given head and inflow rate in the optimization analysis. Many different publications can be found in the literature that have studied the efficiency, cost, and performance of impulse and reaction turbines (Elbatran et al., 2015 and many references therein). This includes advanced numerical modeling with the finite element method. The difference with our work presented herein is (among others) that we do not study the behavior of turbines in isolation, but rather consider their operation and performance in a RoR plant under dynamically varying inflow conditions, and when configured in parallel with other turbines. The technical characteristics of the turbines are discussed next.

2.2.1. Technical characteristics of the turbines

After selecting the suitable turbines for a given installation site, the technical characteristics of each turbine must be examined before a final decision can be made which turbines to use. This includes the specific speed and rotational speed. The specific speed, ω_s, is a dimensionless number that is defined as the ratio of the rotational speeds of two different turbines that are geometrically similar to each other but with differing size of their turbine runners. It can be derived from the laws of similarity and calculated from

$$\omega_s = \frac{1}{60}\frac{\omega\sqrt{O_d}}{(gH_{net})^{\frac{3}{4}}}, \tag{10}$$

where ω (rpm) denotes the rotational speed of the turbine, and the other variables have been defined previously. The multiplication factor of 1/60 is used for unit conservation. The rotational speed in Equation (10) is determined by the frequency, f_e (Hz), of the electric system, and the number of pairs of poles, p (−), of the turbine generator or

$$\omega = \frac{60 f_e}{p} (p = 1, 2, \ldots, 14). \tag{11}$$

However, since a turbine can be coupled with a speed increaser to reach the desired generator speed, the range of the turbine speed is upgraded from a discrete to a continuous function restricted by the upper limit of Equation (11)

$$\omega \leq \omega_{max}, \tag{12}$$

where ω_{max} is the maximum allowable speed of the turbine at $p = 2$ poles.

Table 1 summarizes the ranges of the specific speeds that are used in our simulation experiments presented herein. The listed ranges convey that reaction turbines rotate faster than impulse turbines for a fixed inflow and head. We present purposely dimensionless values so as to be

Table 1
Ranges of the specific speed, ω_s (−) (ESHA, 2004; EUMB, 2009), the values of γ_- and γ_+ and the values of a, b and c in the cost functions for the four different turbines simulated by HYPER. Tabulated values of b and c are rounded to three significant digits. Francis and Kaplan are reaction turbines, whereas Crossflow and Pelton constitute impulse turbines. The symbol μ signifies the number of nozzle used by the Pelton turbine.

Turbine	Range of specific speed	γ_-	γ_+	a	b	c
Pelton	$0.005 \times \mu^{0.5} \leq \omega_s \leq 0.025 \times \mu^{0.5}$	0.1	1.0	17, 692	−0. 364	−0. 281
Crossflow	$0.04 \leq \omega_s \leq 0.21$	0.1	1.0	8, 846	−0. 364	−0. 281
Francis	$0.05 \leq \omega_s \leq 0.33$	0.3	1.0	25, 698	−0. 560	−0. 127
Kaplan	$0.19 \leq \omega_s \leq 1.55$	0.2	1.0	33, 236	−0.583	−0.113

able to compare directly the specific speeds of the Kaplan, Pelton, Francis and Crossflow turbines.

2.2.2. Cavitation

Water that is flowing through a turbine may experience large pressure changes due to rapid variations in the magnitude and direction of the governing forces. These sudden pressure changes may cause the formation of small liquid-free cavities, which can implode near the metal surface of the turbine. The resulting shock wave can erode the turbine, a process known as cavitation. Impulse turbines are hardly vulnerable to cavitation as they convert into mechanical energy the momentum change of the water mass, which rotates at atmospheric pressure. Reaction turbines, on the contrary, are susceptible to cavitation as they convert into rotational energy the pressure and kinetic energy of the flowing water (Pandey and Karki, 2017). The runner and draft tube of such turbines are particularly prone to cavitation, and their deformation and/or disintegration severely compromises turbine performance.

To determine the susceptibility of reaction turbines to cavitation we compute the position of the Francis and Kaplan runner. The runner is comprised of a hub with blades and converts into rotational motion the energy of the flowing water. If the runner position, or so-called admissible suction head, H_s (m), falls below zero then reaction turbines become prone to cavitation as the water vapor pressure may exceed the hydrodynamic pressure. The admissible suction head can be computed using

$$H_s = \frac{P_{atm} - P_v}{\rho_w g} + \frac{V_{out}^2}{2g} - \sigma H_d, \tag{13}$$

where P_v (Pa) denotes the water vapor pressure, V_{out} (m/s) is the turbine's average water outlet velocity, H_d (m) signifies the design head (expected net head) of the proposed plant and σ represents Thoma's coefficient (ESHA, 2004).

The atmospheric pressure, P_{atm} (Pa), at the altitude of the power house, z_{power} (m), can be measured with a barometer or derived from a nearby weather station. Alternatively, as we do in HYPER, we can compute the atmospheric pressure at the power house using the following exponential relationship

$$P_{atm} = P_0 \exp^{(-z_{power}/7000)}. \tag{14}$$

where P_0 (Pa) is the atmospheric pressure at sea level and $z_{power} \geq 0$. Thoma's coefficient depends on the specific speed, ω_s, of the turbine as follows (ESHA, 2004)

$$\sigma_F = 1.2715\omega_s^{1.41} + \frac{V_{out}^2}{2gH_d}, \quad \sigma_K = 1.5241\omega_s^{1.46} + \frac{V_{out}^2}{2gH_d}, \tag{15}$$

where the subscripts F and K denote the Francis and Kaplan turbines, respectively.

The Francis and Kaplan reaction turbines are free of cavitation if the admissible suction head does not fall below zero during operation of the RoR plant. A suitable load and plant design will promote runner life and minimize maintenance costs of the turbines. As the admissible suction head is governed by design parameters and project variables (e.g. Table 2), repeated numerical simulation with HYPER is warranted to determine the extent to which cavitation will take place. This not only helps to determine appropriate maintenance and repair periods, but will also help enhance runner life by suitable operation and loading, and minimize the amount of civil excavation required during initial planning (Maekawa et al., 2003). Indeed, cavitation can be counteracted by migrating the turbine system to a lower elevation. In most cases, this would involve civil excavation to a depth of at least $-H_s$ below the current position of the turbine(s) and would bring about expensive construction costs. HYPER considers explicitly excavation costs in simulation of the energy production and economic profit of a RoR plant. We will describe the computation of costs in section 3.

Table 2
Description of the main project variables of HYPER, including their symbols, units and values.

Variable	Symbol	Value	Units	Reference
Generator efficiency	η_g	0.9	–	ESHA (2004)
Runner position above tailrace	δ_{jet}	1	m	Ramos et al. (2000)
Energy price	e_p	0.073	$/kWh	EMRA (2005)
Penstock cost per ton	c_{ton}	800	$/ton	alibaba.com
Altitude of power house	z_{power}	320/ 900[a]	m	
Total cost coefficient	a	0.25	–	IRENA (2011)
Interest rate	r	9.5	%	Degirmenci (2010)
Life time of the project	L_s	49	year	EMRA (2001)
Resistance term	k_{sum}	1.1	–	Ramos et al. (2000)
Outlet average velocity	V_{out}	2	m/s	ESHA (2004)
O&M cost coefficient	β	2.5	%	IRENA (2011)
EUR/USD exchange rate	ξ	1.1	–	
Minimum environmental flow	q_{md}	0.15/ 0.10[a]	m^3/s	Santolin et al. (2011)

[a] The forward slash separates the values used in case study I and II.

2.2.3. Turbine operation

The design flow and the net head are two key variables that determine the optimal properties and configuration of the hydropower system. The design flow determines the portion of turbine inflow, also called workable flow, that can pass through the turbine, and as such is the maximum flow rate a RoR plant can accommodate. Once the range of potential design flows is obtained from the FDC of the river network, the final decision which turbine to use necessitates nonlinear optimization in which power production is maximized for a given total investment.

Turbines have technical flow constraints and can only operate effectively within certain flow ranges. If only one turbine is installed and used in a hydropower system, then three different operation levels can be distinguished

$$q(t) = \begin{cases} 0 & q \leq q_{min} \\ q & q_{min} < q \leq q_{max} \\ q_{max} & q_{max} < q \leq q_{safety} \\ 0 & q > q_{safety}, \end{cases} \tag{16}$$

where q_{min} is the minimum flow level, also called cutoff flow, below which power generation ceases, q_{max} denotes the maximum flow a

turbine can process, and q_{safety} is the maximum operable flow of the power plant. To protect the power plant against large tail water rises, turbine operation ceases if the runoff exceeds, q_{safety} (Hänggi and Weingartner, 2012). In HYPER, q_{safety} is set equal to Q_2, the river discharge with an exceedance probability of 2%, beyond which turbine operation ceases. The values of q_{min} and q_{max} depend on the design flow and turbine characteristics which may vary from one manufacturer to another. In practice, the values of q_{min} and q_{max} are set as fixed multiple of the design flow, or $q_{min} = \gamma_{-} O_d$ and $q_{max} = \gamma_{+} O_d$. The third and fourth column of Table 1 list the value of γ_{-} and γ_{+} for the Pelton, Crossflow, Francis and Kaplan turbines simulated by HYPER.

As can be seen in Equation (16), a turbine can only operate within a certain envelope of inflows. For this reason it may be advantageous to install several smaller turbines instead. The use of two or more turbines configured in parallel could, at least theoretically, enhance the workable range of inflows, and thus overall efficiency of the RoR plant when confronted with variations in river discharge (Anagnostopoulos and Papantonis, 2007). What is more, the sharing of water between two or more turbines allows for a higher rotational speed, so the turbine torque will be lower leading to a more stable and reliable operation (Penche, 1998). Our numerical model, HYPER, implements the option of two parallel turbines of different size and type. Of course, the choice whether to use one large turbine or two parallel turbines depends on energy production, construction and operational costs. Whatever hydropower system is used, their design and operation should maximize power production for a given financial investment.

Fig. 4 provides a schematic overview of how two turbines working in parallel distribute the available inflow. The first of the two turbines (labeled with subscript "1") is assumed to have the larger design flow. In general, we can discern the following three operational modes in a parallel system consisting of two turbines.

(a/f) The hydropower power system is down due to an insufficiently small or excessively large river discharge.
(b/c) Only one of the two turbines is working
(d/e) Both turbines are working - possibly at maximum capacity

With respect to (a/f) no power is produced if the inflow is below the minimum flow of the second (smaller) turbine, labeled "2", or the flow exceeds the safety limit. With respect to (b/c) the second turbine will generate power if the inflow is larger than its respective minimum flow, and smaller than the minimum flow of turbine one. For inflows between $q_{1\,min}$ and $q_{1\,max}$, the decision which of the two turbines to operate depends on their anticipated production (calculated from Equation (1)). Finally, with respect to (d/e), both turbines are in operation if the current inflow is larger than the maximum flow of turbine one. Both turbines operate at full capacity (load) if the current flow exceeds the sum of their maximum flows (Anagnostopoulos and Papantonis, 2007).

This dual turbine parallel hydropower system is easily coded in MATLAB using the five operational rules defined in Fig. 4. We are currently also investigating how we can generalize the operational rules to hydropower systems consisting of more than two turbines. This could involve a combination of parallel and serially configured turbines.

2.3. Numerical solution of HYPER

The different equations of HYPER are solved numerically using an explicit daily integration time step. This simple Euler scheme suffices in the present application of HYPER as the inflow to the penstock of a RoR plant is controlled directly by river discharge. Dam-based plants, on the contrary, may demand a time-variable integration step (ODE solver) to warrant unconditionally stable simulation of the reservoir storage, spill volumes, net head, turbine inflows and energy production. The output of HYPER consists of daily values of the energy production, $E(t)$, in Equation (1), and the life-time costs and NPV of the plant, of which more later.

Now we have discussed the different building blocks of HYPER, we present in Fig. 5 a detailed flowchart of the model. The gray arrows and decision stencils portray the main program. The blue units signify mathematical functions which compute key variables of interest. The pink slips document the variables that go into the computation of each function's input arguments. Color coding in black, red, purple, and gray is used to distinguish between design parameters, project variables (and model input), universal constants, and simulated variables, respectively. In words, a n-vector with daily values of the river discharge, $q_r = \{q_r(1), ..., q_r(n)\}$, serves as input to HYPER. From each entry of this vector we subtract the value of the residual flow, q_{md}, to yield a n-vector of penstock inflows, $q = \{q_1, ..., q_n\}$ (see Equation (3)). Then at each time, t (days), HYPER computes the net head, $H_{net}(t)$, by subtracting from the gross head (known constant), the friction losses in the penstock and singular losses in the conveyance system (see Equation (4)). Both these losses depend upon the penstock diameter, D. Next, the value of $H_{net}(t)$ and the design flow, O_{dj}, determine the rotational and specific speed of the T turbines (Equations (10) and (11)), where $j = \{1, ..., T\}$. For reaction turbines (e.g. Francis and Kaplan), HYPER computes as well the suction head, H_s (see Equation (13)), to combat cavitation and account for this in the costs. Then, the operational rules of Fig. 4 are used to determine the water inflow to single, $T = 1$, and dual, $T = 2$, turbine systems. The ratio of the inflow and design flow is then used to compute the efficiency of each turbine using the efficiency curves depicted in Fig. 2. At this point, all variables of Equation (1) are known, and HYPER can, thus, compute the energy production of the plant between time $t - 1$ and t. This series of successive steps is repeated until all entries of the discharge vector have been processed and t equals n. In the last two functions, HYPER computes the life-time costs and NPV of the RoR plant, details of which are given in the next section.

The performance of the RoR plant depends critically on the values of the design parameters and the choice of turbine system. HYPER

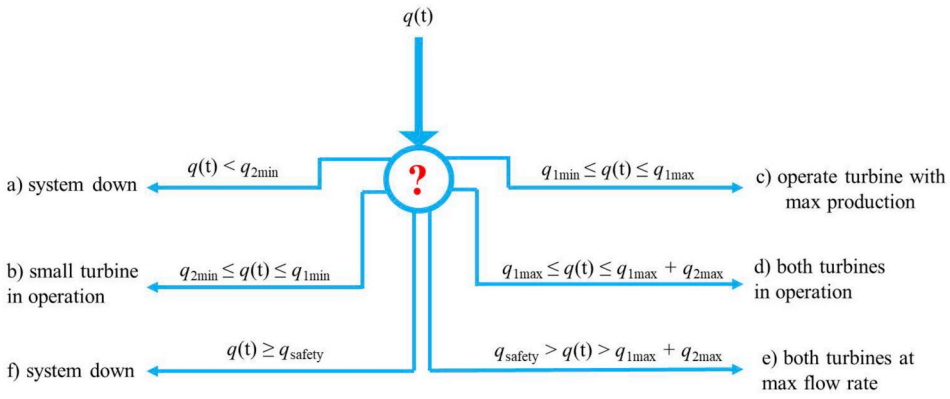

Fig. 4. Schematic overview of the operational rules of a parallel hydropower system composed of $T = 2$ turbines.

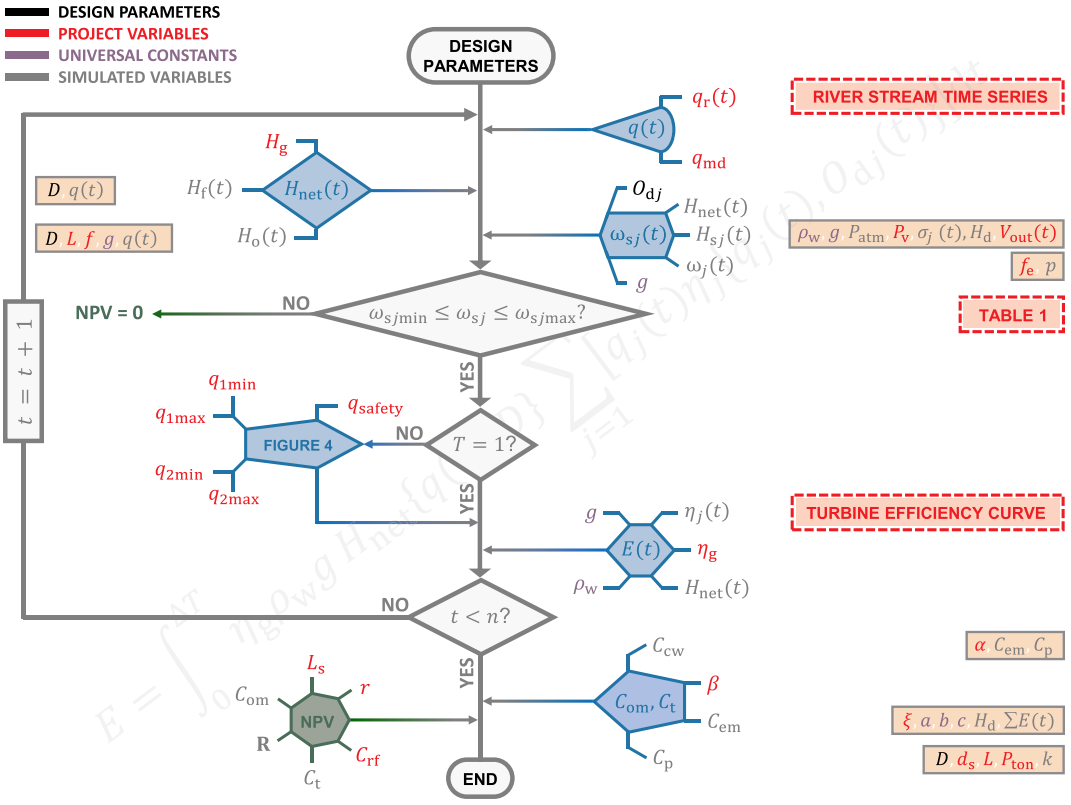

Fig. 5. Detailed flowchart of HYPER. The gray sequence of arrows and conditions in the center of the chart symbolizes the flow of the main program. The blue stencils signify mathematical operators, so-called subroutines or functions, which compute key variables of interest. We list separately the input arguments of each subroutine and document in the pink slips the variables the input arguments themselves directly depend on. Color coding is used to differentiate between design parameters (in black), project variables and/or model inputs (red), universal constants (purple) and simulated variables (gray). Once the program has cycled (iterated) through all n entries, $q_r = \{q_r(1), ..., q_r(n)\}$, of the discharge record, HYPER determines, in a penultimate function call, the total and operation and maintenance costs of the proposed plant. These values serve as input to the last subroutine (green heptagon) which computes the NPV of the RoR plant for the respective design parameters specified by the user. In practice, the last function returns an array of different output arguments and performance statistics. (For interpretation of the references to color in this figure legend, the reader is referred to the Web version of this article.)

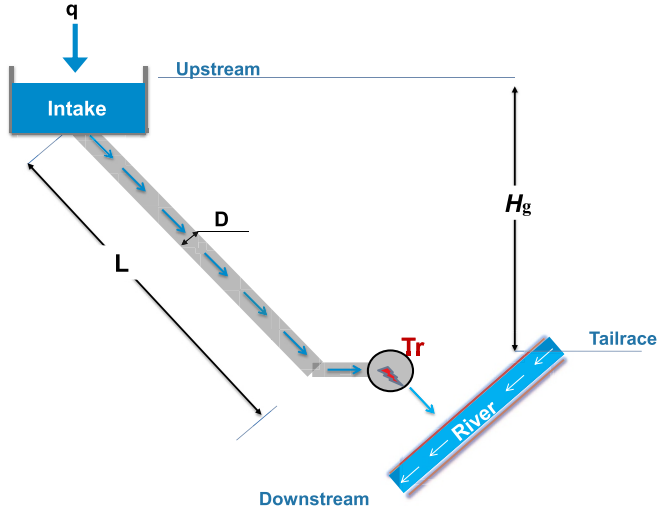

Fig. 6. Schematic overview of a single turbine RoR hydropower plant. The penstock of length L and diameter D carries water from the intake to the turbine (in red). The gross head, H_g, is determined by plant design and determines in large part turbine selection, energy production and the necessary investment and maintenance costs of the electromechanical equipment. The object Tr represents the turbine. (For interpretation of the references to color in this figure legend, the reader is referred to the Web version of this article.)

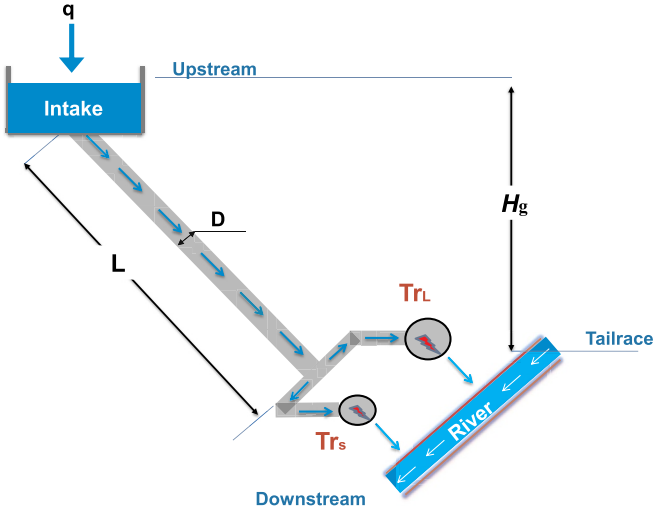

Fig. 7. Schematic representation of a dual hydropower system with $T = 2$ turbines configured in parallel. Tr_L and Tr_S signify the large and small turbine, respectively.

includes a built-in optimization module that can be used to optimize the plant design and hydropower system for a given monetary investment. This component of the model will be discussed in the next section.

3. Nonlinear optimization and objective functions

This section discusses the optimization module of HYPER. This built-in module is easy to execute and enables users to maximize the RoR plant's power production, economic profit or NPV by optimizing relevant design and project variables. In this paper, we focus our attention on the design parameters of the RoR plant. This involves the penstock diameter, D, and the design flow, O_{d1}, of the turbine. For a parallel hydropower system composed of two side-by-side turbines, this includes as well the design flow, O_{d2}, of the second turbine. These design parameters determine the penstock thickness, k, suction head, H_s, and rotational speed, ω_1 and/or ω_2, of the turbines.

The built-in optimization module of HYPER maximizes the NPV of the RoR plant and returns to the user a Table with optimal design parameters for the Francis, Pelton, Kaplan and Crossflow turbines depicted in Figs. 2 and 3. This analysis reports as well the optimal design parameters of dual hydropower systems. HYPER limits attention to parallel systems with two turbines of the same type as this simplifies considerably practical maintenance and operation, and manifold design (distributes the water among the two turbines).

3.1. The optimization algorithm

We use a meta-heuristic, called differential evolution, (DE) to determine the optimal design parameters. DE is a derivative-free, population-based, global optimization algorithm that is well suited to the task of finding optimal solutions in search spaces with non-ideal response surfaces (Storn and Price, 1997; Price et al., 2005). DE does not require users to make assumptions about the search space other than the ranges of the parameters, and can handle non-continuous and noisy optimization problems. Classic optimization methods such as gradient-descent and quasi-Newton methods can be devised, yet these methods are sensitive to local optima in their pursuit of the global optimum. Furthermore, these local search methods cannot handle well a very large number of parameters. Thus, we purposely implement DE in anticipation of the application of HYPER to RoR plants with a much large number of decision and design variables.

The DE method starts out with an initial population, $\mathbf{X}_{(1)} = \{\mathbf{x}^1_{(1)},...,\mathbf{x}^N_{(1)}\}$, of N parent parameter vectors, $\mathbf{x}^i_{(1)} = \{x^i_{(1)1},...,x^i_{(1)d}\}$, drawn at random from the prior search ranges, $\mathbf{x}^i_{(1)} \in \mathbf{X}_{(1)} \subseteq \mathbb{R}^d$, where d denotes the dimensionality of the search space, and $i = \{1,...,N\}$. Next, we compute the NPV for each vector of design parameters of $\mathbf{X}_{(1)}$ and store the resulting values in the N-vector, $\mathbf{f} = \{\text{NPV}(\mathbf{x}^i_{(1)}),...,\text{NPV}(\mathbf{x}^N_{(1)})\}$. Each parent of the population now produces offspring as follows. If $\mathscr{A}$ is a subset of m-dimensions of the original parameter space, $\mathbb{R}^m \subseteq \mathbb{R}^d$, then the child, $\mathbf{z}^i$, of the ith parent, $i = \{1,...,N\}$, at generation $j = \{2,...,J\}$ is computed using (Storn and Price, 1997; Price et al., 2005)

$$\begin{aligned} \mathbf{z}^i_{\mathscr{A}} &= \mathbf{x}^{r_1}_{(j-1),\mathscr{A}} + \lambda_{\text{DE}}\left(\mathbf{x}^{r_2}_{(j-1),\mathscr{A}} - \mathbf{x}^{r_3}_{(j-1),\mathscr{A}}\right) \\ \mathbf{z}^i_{\neq\mathscr{A}} &= \mathbf{x}^i_{(j-1),\neq\mathscr{A}} \end{aligned} \tag{17}$$

where the integers r_1, r_2, and r_3 are selected without replacement from $\{1,...,i-1,i+1,...,N\}$, and $\lambda_{\text{DE}} \in (0, 2]$ is an algorithmic variable that controls the diversity and spread of the offspring. The children are compiled in an offspring population, $\mathbf{Z} = \{\mathbf{z}^1,...,\mathbf{z}^N\}$, and their objective functions are calculated and stored in the N-vector, $\mathbf{g} = \{\text{NPV}(\mathbf{z}^i),...,\text{NPV}(\mathbf{z}^N)\}$. Now a pairwise comparison of child and parent is used to determine whether to accept the offspring or not. If $g(i) \geq f(i)$, then the ith child replaces the parent, $\mathbf{x}^i_{(j)} = \mathbf{z}^i$ and $f(i) = g(i)$, otherwise the ith child is discarded and the parent moved to the new population, $\mathbf{x}^i_{(j)} = \mathbf{x}^i_{(j-1)}$. If the maximum number of generations, J, has not been reached, go back to Equation (17), otherwise stop, and return as solution to the optimization problem the parent with the highest value (or lowest, if appropriate) of the NPV in the final population, $\mathbf{X}_{(J)}$. We refer readers to Storn and Price (1997) for a detailed description of the algorithm.

The number of dimensions, m, stored in $\mathscr{A}$ ranges between 1 and d and depend on the actual crossover value used. In our calculations we use a crossover value, $\tau = 0.8$, and determine the dimensions of $\mathscr{A}$ as follows. Each time a child is created, we sample a vector, $\mathbf{e} = \{e_1,...,e_d\}$, with d random labels from a standard multivariate uniform distribution, $\mathbf{e} \sim \mathscr{U}_d(0, 1)$. All dimensions, k, for which $e_k \leq \tau$ are stored in $\mathscr{A}$ and span the search space of the child. In the case that $\mathscr{A}$ is empty, one dimension of $\mathbf{x}_{(j-1)}$ will be sampled at random. This simple randomized strategy activated when $\tau < 1$ constantly introduces new search directions outside the subspace spanned by the current parent population and enables single-parameter updating, multi-parameter sampling (a group of parameters), and full-dimensional search (all dimensions). In practice, it may happen that the offspring produces specific speeds that are outside the range documented by the turbine manufacturer. Such solutions are undesirable and therefore penalized with a zero value of the NPV objective function (see Figs. 1 and 5). This will promote convergence to physically realistic design parameters.

3.2. Objective function

Once the technical feasibility of a site has been established, a key issue that remains is to determine the economic value of the hydropower project. The total development costs of a RoR plant is made up of three main balance-sheet items, including the cost of the civil works, C_{cw}, electric and hydro-mechanical equipment, C_{em}, and penstock, C_p. The yearly revenue of a RoR plant, R_a, is simply equivalent to the net difference between the cumulative amount of money made per time unit (year) from selling the produced energy (electricity), and the yearly operation and maintenance cost, C_{om}. Part of the revenue is used to pay off the initial investment, possibly inflated with multi-year interest. As most hydropower plants have relatively high installation costs and considerably lower operation and maintenance costs, a large portion of the projects monetary budget will be exhausted during the construction stage. The energy production of the RoR should hence be optimized carefully to reach the earning potential of the plant and guarantee long-term operation and longevity.

The proposed objective function measures the net balance of earnings (income) and expenses (expenditures) and helps determine whether the RoR plant is economically feasible and profitable or not. This metric, also referred to as the NPV is an economical index used to determine the profitability of a prospective monetary investment. The NPV equals the net difference between the cumulative sum of all discounted cash inflows generated by the power plant (also called assets) and the total expenditures (liabilities) incurred during the lifetime of the project. To be profitable, the RoR plant should have a NPV value greater than zero.

Different empirical equations have been proposed in the hydropower literature to calculate the investment and maintenance costs of a RoR plant (Gordon and Penman, 1979; Voros et al., 2000; Kaldellis et al., 2005; Aggidis et al., 2010; Singal et al., 2010). Unfortunately, most of these equations are not readily applied to a new hydropower project as they are either site specific, applicable only to certain regions in the world, or representative for past market conditions and/or prices. We next discuss the lifetime expenditures of the RoR project, and detail the set of equations HYPER uses to determine separately the price for operation and maintenance and the costs of the electromechanical equipment, penstock, and civil works.

The electromechanical equipment (turbine, generator, and power transformer) are most cost intensive. We compute the cost of the electromechanical equipment, C_{em} ($), using the following equation (Ogayar and Vidal, 2009)

$$C_{em} = a\xi(P/1000)^{(b+1)}(H_d)^c, \tag{18}$$

where ξ signifies the exchange rate of Euro (€) to US dollar ($), P (MW) is the installed capacity of the RoR hydropower plant (see Equation (2)), and a, b, and c are coefficients whose values are reported in Table 1 for each of the four turbines simulated by HYPER. The multiplication factor of 1/1000 converts the units of P from MW to kW. Note that Ogayar and Vidal (2009) do not specify an equation for the cost of the electromechanical equipment of the Crossflow turbine. The listed values of a, b, and c for this turbine honor RE (2004) that the electromechanical costs of the Crossflow turbine are about half of those of the Pelton turbine for the same design head (RE, 2004).

The cost of the penstock, C_p ($), is another major project expense and is calculated as follows

$$C_p = \pi(D + 2k)kd_sLc_{ton}, \tag{19}$$

where D, k and L signify the diameter, thickness and length of the penstock in units of meters, respectively, d_s (ton/m^3) denotes the steel density and c_{ton} ($/ton) is the penstock cost per ton weight.

The cost of the civil works, C_{cw} ($), is perhaps most difficult to determine as it depends on a large number of different factors, including the characteristics of the river stream (discharge and variations thereof), the anticipated capacity of the RoR plant, the local price for labor and materials, and the accessibility, topography and underlying geology of the installation site and its distance to existing infrastructure and transmission lines. What is more, reaction turbines may demand excavation to negate cavitation. The total costs of the civil works will be negligible for an existing dam-based plant but may amount up to 60% of the initial investment for a new RoR project (IRENA, 2011). We use the following equation for the total costs of the civil works

$$C_{cw} = \alpha(C_{em} + C_p), \tag{20}$$

where α is a unitless coefficient, the so-called site factor, that can take on values between 0 and 1.5 (IRENA, 2011).

The yearly maintenance and operation cost, C_{om}, of the hydropower plant is directly proportional to the cost of the electromechanical equipment, C_{em} (Gordon and Penman, 1979; Voros et al., 2000; Kaldellis et al., 2005; Hosseini et al., 2005; IRENA, 2011), and calculated using

$$C_{om} = \beta C_{em}, \tag{21}$$

where β is a unitless coefficient whose value ranges between 0.01 and 0.04 (IRENA, 2011).

Economic analysis of a RoR hydropower plant should include explicit recognition of the life-span and depreciation of the hydropower plant and electromechanical equipment. Most of the concrete structure of the plant will be easy to repair or upgrade at time of aging. The wear and tear of the hydropower generating system is more difficult to ascertain and demands costly maintenance to mend and/or replace deficient parts and/or substitute components that may have become obsolete by more efficient equipment. Turbines and other components of the electromechanical system have an anticipated life-span, L_s, of about 25 years. The value of this equipment at the time of purchase is approximately equal to the costs of renovation and reconstruction 25 years later (Hosseini et al., 2005). The total monetary investment, C_t ($), of a RoR plant with a life time of 50 years can be calculated as follows

$$C_t = C_{cw} + 2C_{em} + C_p. \tag{22}$$

Now we have defined the expenditures, we can now compute the NPV of the plant by subtracting the life-time costs from the cumulative revenues of the produced electricity.

If we conveniently assume the RoR plant to be connected to a central electrical grid then all the hydro-electrical energy produced by the turbines can be stored, used and sold. This simplification avoids HYPER from having to simulate human use of the electrical-grid with load matching to store excess electrical power during low demand periods for release as demand rises. Thus, if we assume an infinite energy demand, then the NPV can be computed using

$$\text{NPV} = \left[\frac{R_a(1) - C_{om}}{1 + r(1)} + \frac{R_a(2) - C_{om}}{(1 + r(2))^2} + \ldots + \frac{R_a(L_s) - C_{om}}{(1 + r(L_s))^{L_s}} - C_t\right]C_{rf} \tag{23}$$

where $R_a = \{R_a(1) \ldots, R_a(L_s)\}$ and $r = \{r(1), \ldots, r(L_s)\}$ are L_s-vectors with the annual plant revenues in dollars and the annual interest rate in %, respectively, and C_{rf} $(-)$ signifies the capital recovery factor.

If we conveniently assume a constant interest rate, r, and energy price, e_p ($/kWh), over the life time, L_s, of the project, then the yearly revenue of the RoR plant simplifies to a fixed multiple of the annual energy production, E_a (kWh), as follows

$$R_a(l) = e_p E_a(l) \qquad (l = 1, 2, \ldots, L_s), \tag{24}$$

where $E_a(l)$ is equal to the sum of the daily values of $E(t)$ in Equation (1) computed by HYPER for year l, and the capital recovery factor equates to

$$C_{rf} = \frac{r(1 + r)^{L_s}}{(1 + r)^{L_s} - 1}. \tag{25}$$

We now have all ingredients to compute the annual NPV of the plant. If we assume a constant annual production of power

$$\bar{E}_a = \frac{1}{L_s}\sum_{l=1}^{L_s} E_a(l), \tag{26}$$

and inflow of cash, $\bar{R}_a = e_p\bar{E}_a$ ($), then Equation (23) simplifies to

$$\text{NPV} = \left[\frac{1}{r}(\bar{R}_a - C_{om})(1 - (1 + r)^{-L_s}) - C_t\right]C_{rf}, \tag{27}$$

which after further manipulation leads to

$$\text{NPV} = \bar{R}_a - C_{om} - C_t C_{rf}. \tag{28}$$

4. Case studies and results

We now illustrate the main results of HYPER using two illustrative case studies. These two examples cover a relatively wide range of heads and river discharges (and their variability) for which different turbines (and their combinations in parallel) will be deemed most effective (Fig. 3). For example, the Kaplan and Crossflow turbines are most effective at heads smaller than 20 m, whereas Francis and Pelton are designed to accommodate (much) larger heads. In each study, we summarize the power production and NPV of the RoR plant using long records of daily discharge values (see Fig. 8) and, report the results for the DE optimized design parameters for operation with a single turbine (see Fig. 6) and two turbines configured in parallel (see Fig. 7).

Table 2 summarizes the main project variables of HYPER (parameters), their default values and units. These variables are held constant (not optimized) in both case studies. The numerical results of HYPER depend, of course, on the values of the project parameters. Insofar possible literature references are provided to justify the default settings of the different variables. The energy price, e_p (¢/kWh), site factor, α $(-)$, interest rate, r (%), and operation and maintenance cost coefficient, β (%) (Ramos et al., 2000; Kaldellis et al., 2005), exert a large control on the NPV and energy production simulated by HYPER. Their default values will, thus, affect the optimized values of the design parameters of the RoR plant. For example, it should be intuitively clear that the value of the NPV is determined by the interest rate. A significant increase of r would decrease the NPV of the RoR plant and result in lower optimized values of the design parameters (a smaller and less expensive plant) to reduce (among others) the enhanced payments for the initial investment. The same will happen if the energy price, e_p, drops or the cost of the penstock, C_p, increases and the revenues of the

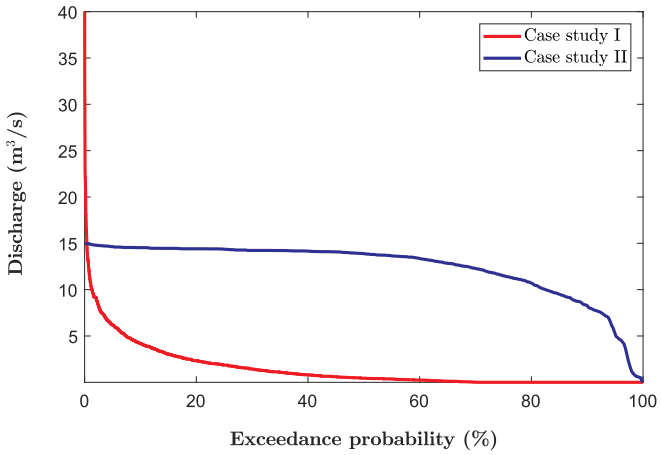

Fig. 8. Plot of the *daily* flow duration curves used in the first (red) and second (blue) case study. The FDC depicts graphically the relationship between the magnitude of the discharge (on *y*-axis) and its exceedance probability (on *x*-axis). Thus, in 80% of the days the discharge of the blue river will exceed 10 m^3/s. This equates to 300 days per year. It is evident from the plotted FDCs that the two rivers exhibit a quite different discharge regime. This should have important consequences for the design of each RoR plant. (For interpretation of the references to color in this figure legend, the reader is referred to the Web version of this article.)

RoR plant decrease. On the other hand, if the values of α and/or β decrease then this reduces the life-time cost of the RoR plant and the DE algorithm should return larger values of the optimized design parameters.

In this paper, we limit attention to optimization of the design parameters of the RoR plant using four different turbines configured in parallel or not. Bayesian analysis can be used to quantify the effect of each project parameter of Table 2 on the optimized design (parameters) of the RoR plant. Alternatively, one could use sensitivity analysis to analyze the impact of each project parameter on the simulated results of HYPER, yet this is beyond the scope of the present paper, and will be investigated in due course.

4.1. Case study I

Our first case study involves the analysis of a proposed RoR hydropower plant in Turkey. As this project is still at the planning phase, we cannot divulge specific information about the plant, river, and installation site. Nevertheless, we present in Fig. 8 the FDC (red line) of the river of interest, as this suffices for HYPER. The discharge fluctuates considerably between values of 0 and 40 m^3/s, with mean flow of about 1.5 m^3/s. In our calculations, we assume a generator efficiency, $\eta_g = 0.9$, gross head, $H_g = 133.95$ (m) and length of the penstock, $L = 1600$ (m). Under these conditions, the average annual energy production should, at least in theory, equate to about 15 GWh using either the Francis, Pelton or Crossflow turbines or combinations thereof (Fig. 3). We optimize the design parameters of the RoR plant with the DE algorithm using a population size of $N = 10$ individuals in combination with $J = 150$ generations.

Fig. 9 displays trace plots of the optimized design parameters for the NPV objective function assuming RoR plant operation with a single Crossflow turbine (top row: A,B,C) or two Francis turbines configured in parallel (bottom row: D,E,F,G). The last panel at the right-hand-side plots the evolution of the optimized NPV values of the parent population. The most important results are as follows. First, about 50 generations with the DE algorithm appears sufficient to converge adequately to a single optimum solution. Repeated trials with DE provide the same optimum design parameter estimates, irrespective of the size of the initial population size. Moreover, our results are confirmed separately by the Nelder-Mead simplex algorithm, a derivative-free local optimizer. This inspires confidence in the ability of the DE algorithm to solve for the design parameters of a RoR plant. Second, the use of two parallel configured Francis turbines enhances the net profit (NPV) from 127 (single turbine) to 199 (K$), an increase of almost 60%. Apparently, the use of two Francis turbines increase the range of workable flows and enables more effective power production when confronted with highly variable stream flows. This confirms earlier findings of Anagnostopoulos and Papantonis (2007). Third, the optimized value of the diameter of the penstock of around 1.2 m is rather similar for both cases, whereas the design flows of the turbines differ substantially. Indeed, when using a single turbine for power production, the optimized design flow equates to about 5.28 m^3/s. For the parallel case, the optimum design flows are equivalent to 4.58 (first, bigger turbine) and 1.02 (second, smaller turbine). Thus, the use of two Francis turbines allows for a smaller design flow of the second turbine and hence accommodates more easily a range of inflows.

Table 3 lists the optimized values of the design parameters for all single and parallel turbine configurations of the RoR plant. The first four columns list the name(s) of the turbine(s) used, the optimized value of the NPV (K$) and corresponding values of the installed capacity, P (MW) in Equation (2) and annual average power production, $\bar{E}_a$ (GWh), in Equation (26). This is followed by the optimized values of the penstock diameter and the design flow of each turbine. The last four columns tabulate the rotational speed of the turbine(s), admissible suction head, and thickness of the penstock, respectively. These variables are derived from the optimized design parameters using Equations (9), (11) and (13), respectively.

The use of two turbines not only significantly enhances the net profit (NPV) of the RoR plant, but also dramatically enhances the annual power production from about 9 GWh to approximately 11 GWh. This amounts to a production increase of about 20%. Altogether, the parallel configuration of two Francis turbines (large and small) produces the largest value of the NPV for given head and river discharge. A close contender would be the Crossflow - Crossflow system, as this configuration maximizes the installed power and has the second largest NPV. For the present FDC and installation site, the Francis - Francis turbine system is preferred.

The annual power production of about 10.21 GWh is considerably lower than the maximum achievable value (theoretical) of 15 GWh derived previously for a ”perfect” turbine without any hydraulic losses in the conveyance system of the hydropower system. In practice, the RoR plant efficiency can therefore only reach up to about 65–73% of the theoretical maximum attainable productivity.

The daily power production of the parallel system is considerably larger than that of the single Francis turbine configuration simply because the inflows are lower than the minimum operable flow. We conclude that a single turbine is unable to accommodate effectively a large range of streamflows. A parallel configuration with two or more turbines is hence preferred as such system enhances the range of workable flows and thus can sustain energy production in the presence of highly variable streamflows. However, a little increase in the electricity price may make the Pelton-Pelton combination more profitable instead. This combination extracts about 73% of the maximum attainable power.

4.2. Case study II

The second case study adopts the FDC of Santolin et al. (2011), which is depicted in blue in Fig. 8. The discharge of this watershed is quite constant compared to the first study, and fluctuates between values of 0 and 15 m^3/s, with mean flow value of about 12 m^3/s. We assume a generator efficiency, $\eta_g = 0.9$, penstock length, $L = 85$ m, and set the value of the gross head, H_g, equal to the value of 41.5 m used by Santolin et al. (2011). These values should, at least in theory, produce an annual energy of about 38 GWh. Furthermore, for $H_g = 41.5$ m and

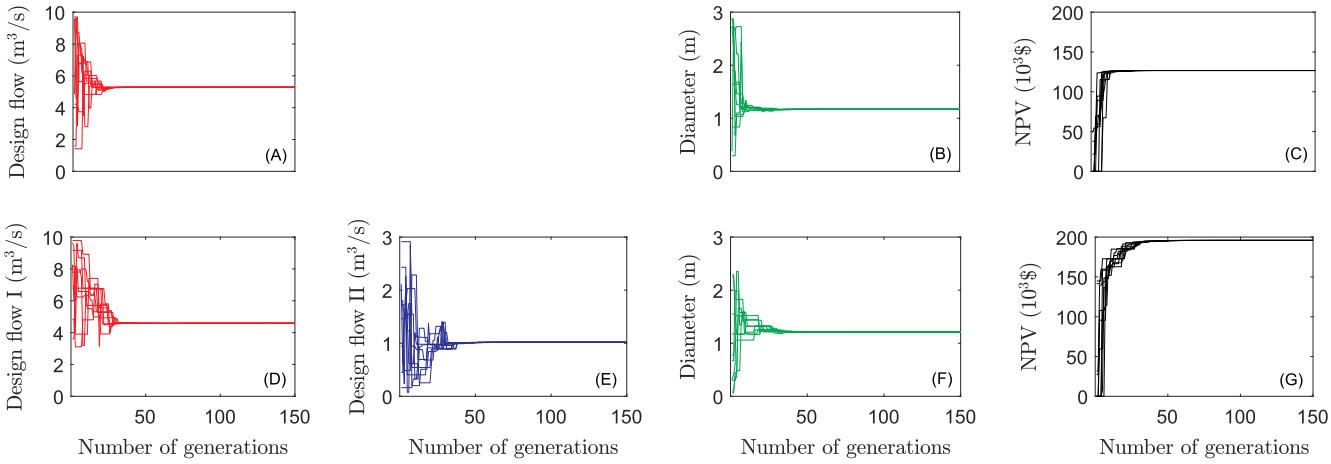

Fig. 9. Case study I: Values of the design parameters as function of the number of generations with the DE algorithm. The three graphs in the top panel portray the results of the Crossflow turbine, whereas the four graphs in the bottom panel illustrate our findings for a dual hydropower system composed of two parallel configured Francis turbines.

Table 3
Case Study I: Optimized values of the net present value (column 2) for single and dual turbine systems derived from the built-in DE algorithm using maximization of the NPV with $J = 150$ generations. For each turbine type and configuration we report separately the optimized values of the design flow(s), O_{d1} and/or O_{d2}, and penstock diameter, D, and list corresponding values of the installed capacity, P (MW), annual average power production, $\bar{E}_a$ (GWh), rotational speed, ω_1 and/or ω_2 (rpm), admissible suction head, H_s (m), and minimum penstock thickness, k (m). The red and blue font color single out the best results for the NPV and annual power production, respectively.

Turbine system	NPV	P	$\bar{E}_a$	O_{d1}	O_{d2}	D	ω_1	ω_2	H_s	k
	(K$)	(MW)	(GWh)	(m^3/s)	(m^3/s)	(m)	(rpm)	(rpm)	(m)	(cm)
Francis	35	3.67	7.42	3.84	–	1.08	750	–	1.73	1.5
Pelton	98	4.55	9.56	4.88	–	1.14	250	–	–	1.5
Crossflow	127	4.90	8.92	5.28	–	1.17	1000	–	–	1.5
Francis - Francis	199	5.24	10.21	4.58	1.02	1.21	750	1500	0.67	1.5
Pelton - Pelton	158	5.58	10.91	4.97	1.17	1.21	250	500	–	1.5
Crossflow - Crossflow	195	5.94	10.25	5.00	1.57	1.23	1000	1500	–	1.5

a mean river flow of 12 m^3/s, the turbine chart in Fig. 3 dictates use of the Francis, Kaplan and Crossflow turbines. Henceforth, those three turbines will be considered in our numerical experiments with HYPER. The design parameters are optimized with the DE algorithm using a population size of $N = 10$ individuals in combination with $J = 150$ generations.

Fig. 10 displays trace plots of the optimized design parameters using a hydropower system composed of a single Francis turbine (top row: A,B,C) or two parallel Francis turbines (bottom row: D,E,F,G). The optimized NPV value of both turbine configurations is about equal and amounts to 2.33 and 2.32 (M$) for the single and parallel hydropower systems respectively. This rather insignificant gain (actually a small loss) of the dual turbine system is not surprising. The turbine inflow at this particular site is nearly constant, and hence a single turbine suffices to maximize energy production. A second turbine only marginally increases the energy production while adding additional costs to the

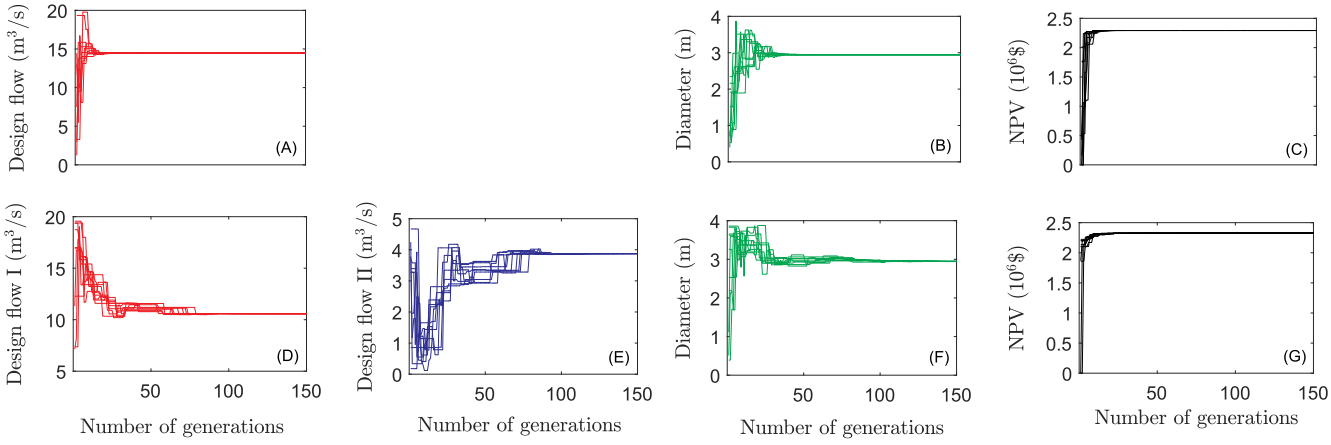

Fig. 10. Case study II: Evolution of the design parameters of HYPER using global optimization with the built-in DE algorithm. The graphs in the top panel present the design flow, penstock diameter and NPV of a hydropower system composed of a single Francis turbine, whereas the bottom four graphs display traceplots of the design flows, penstock diameter and NPV for a dual hydropower system with two parallel configured Francis turbines.

Table 4
Case Study II: The optimized net present value of single and dual (parallel) turbine systems and corresponding values of the installed capacity, P, annual average power production, $\bar{E}_a$, design parameters, O_{d1}, O_{d2} and D, and related variables, ω_1, ω_2, H_s and k, derived from maximization of the NPV with the DE algorithm using $J = 150$ generations. The red and blue font color single out the best results for the NPV and annual power production, respectively.

Turbine system	NPV	P	$\bar{E}_a$	O_{d1}	O_{d2}	D	ω_1	ω_2	H_s	k
	(M$)	(MW)	(GWh)	(m^3/s)	(m^3/s)	(m)	(rpm)	(rpm)	(m)	(cm)
Francis	2.33	4.79	35.47	14.45	–	2.95	375	–	0.80	2.5
Kaplan	2.24	4.83	35.20	14.55	–	2.94	333	–	1.22	2.5
Crossflow	2.03	4.90	31.92	14.743	–	2.90	272	–	–	2.5
Francis - Francis	2.32	4.80	35.94	10.58	3.88	2.95	428	750	0.40	2.5
Kaplan - Kaplan	2.25	4.86	35.33	13.59	1.07	2.94	428	600	0.23	2.5
Crossflow - Crossflow	2.03	4.89	31.96	14.74	0.1	2.89	272	3000	–	2.5

construction and maintenance of the hydropower system. In other words, the necessary capital investment and maintenance costs of the second turbine exceed revenues from the incremental power production. Further evidence for this finding is found in Table 4, which reports for each turbine type, individual and in parallel, the optimized NPV (M$) and corresponding values of the installed capacity, P (MW), in Equation (2) and annual average power production, $\bar{E}_a$ (GWh), in Equation (26), design parameters, rotational speed, admissible suction head, and penstock thickness. These last four variables are computed from Equations (9), (11) and (13), respectively. We reiterate that the listed design parameters maximize the NPV. Altogether, the Francis turbine alone can deliver up to 90% of the maximum attainable power, whereas the Francis - Francis combination achieves an efficiency of about 94%. Tables 3 and 4 emphasize the need for a coupled modeling and optimization framework to determine accurately the most profitable and/or productive turbine system for a given river.

In the interpretation of the results in Table 4, it is important to be aware of the negative dependency between the rotational speed of a turbine and the diameter of the runner. The larger the rotational speed of a turbine the smaller the required diameter of the turbine runner, and thus overall size of the turbine for a given design flow. The optimized rotational speed of the Francis turbine is 375 rpm, whereas this value changes to values of 428 and 750 rpm for a hydropower system with two Francis turbines configured in parallel. Hence, it may still be advantageous to use two Francis turbines system instead of one large turbine, even if the net benefit of such parallel system is rather marginal. From all single turbines, the Francis turbine is most effective because of the rather uniform inflows.

We conclude that a single turbine is sufficient for river systems that produce a nearly constant discharge during the year. The parallel operation of two or more turbines allows for a smaller diameter of the runner blades, and enables electricity production during almost the entire year. The highest NPV in the present study is obtained with a Francis turbine operating at a design flow rate, O_d, of 14.45 m^3/s and requiring no excavation.

5. Graphical user interface (GUI)

For those that are not too familiar with hydro-electric modeling and simulation, we have developed a graphical user interface (GUI) of HYPER. Fig. 11 presents a screen shot of the GUI, which, as you will notice, includes the settings of the DE optimization algorithm as well. The version of HYPER with built-in optimization algorithm is coined HYPER optimizatION, abbreviated $HYPER_{ION}$, the name of which was also given in the early 1980s to the first portable IBM computer.

The left panel (in cyan) provides a list with project variables. These values can be changed by the user depending on the properties of the local installation site, and anticipated design and economic variables of the RoR plant. After all variables have been given a value and the discharge data (with extension.txt) has been loaded, the user can select whether to operate the RoR plant with a single turbine or two turbines configured in parallel. In the current version of the GUI, the user does not have the option to preselect a certain turbine or combination of turbines - all four turbines (and their combinations) are separately considered in the optimization analysis with DE, the settings of which are defined in the purple box in the bottom right corner. This box allows the user to specify values for the population size and number of generations in the DE algorithm, and the feasible ranges of the most important design parameters considered in the literature in optimization analysis of RoR plants. The dark red box labeled "Objective Function" allows the user to select which objective function to maximize, and is currently limited to the power production, net profit, internal rate of return (IRR) and pay-back (PB) of the plant. These latter two objectives have not been considered in the present study but will be studied in future publications. Finally, the user has the option to specify their own efficiency curves for the Kaplan, Francis, Crossflow, and Pelton turbines. These curves are loaded from individual text files supplied by the user (name of turbine with extension.txt) and consist of two columns that list the ratio of q and O_d and the corresponding turbine efficiency. If such curves are not available, then the user of HYPER can resort to the default curves used in the preset study. In any case, a sufficient range of inflow values is required to be able to simulate adequately the production of power under different inflow values.

The GUI is designed especially to simplify numerical simulation with HYPER. We anticipate changes to the GUI in the coming years to satisfy users, and further enhance the number of options and flexibility of use. For instance, we can extend the optimization analysis (and thus DE box) to not only include the design parameters but also decision variables that determine RoR plant operation. Moreover, we will include the option of three parallel turbines, and simulation of additional turbines beyond the four used currently. What is more, we will also include the option of multi-criteria optimization involving the use of two or more objective functions simultaneously. This will give rise to a Pareto front, and can help decision makers to determine the best design and/or operation for given site conditions.

The IRR and PB objective functions are not considered in the present study, but will be considered in future work involving multiple objective optimization with AMALGAM (Vrugt and Robinson, 2007). The IRR objective function quantifies risk, whereas the PB metric defines the number of years before the construction and design costs of the RoR plant are earned back and the plant is profitable.

The output of the GUI consists of a Table which lists the optimal design parameters, energy produced (kWh) and total cost ($M) of the RoR plant for a single turbine or two turbines configured in parallel. The results for all turbines (and their combinations) are listed. The symbols used match those used for different variables in the present paper. It is evident from the results that the use of two turbines in parallel enhance the power production with about 10–20% depending on the exact turbine combination. The investment costs, however also increase. This warrants a detailed analysis of their trade-offs with AMALGAM.

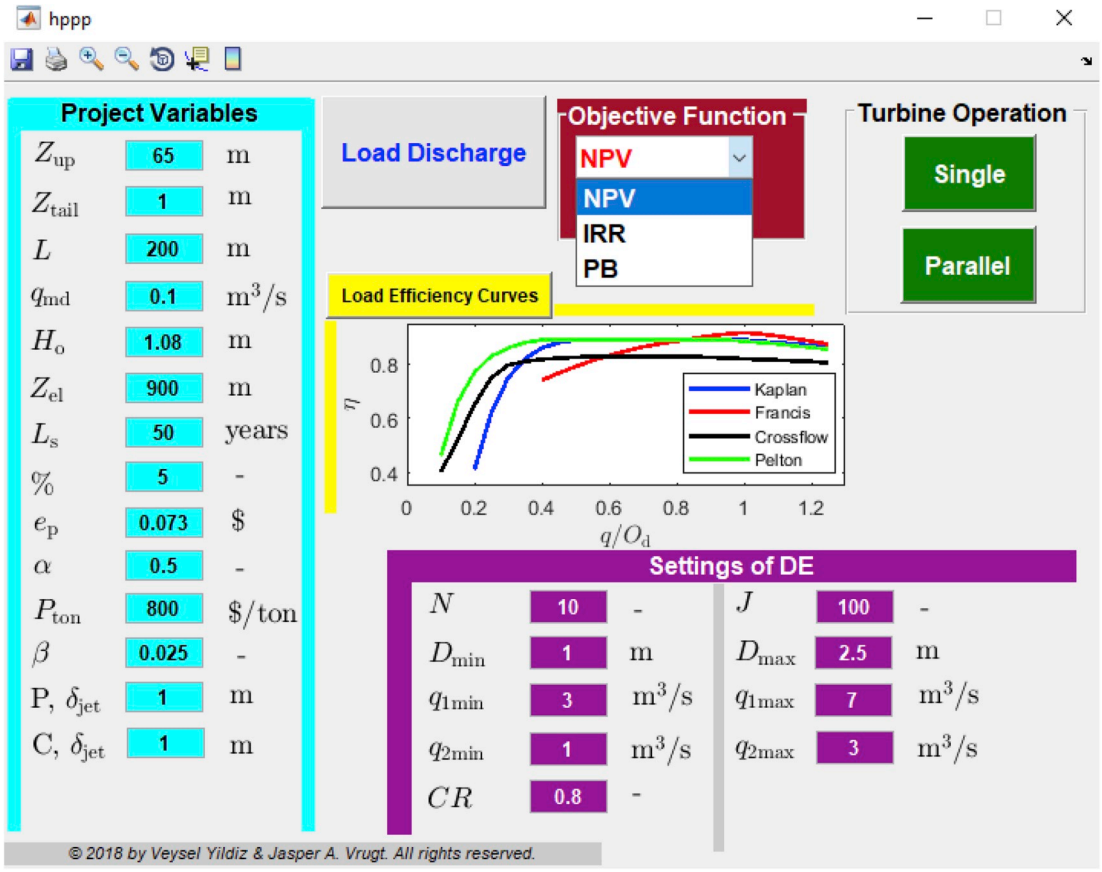

Fig. 11. Screen shot of the graphical user interface of HYPER. A detailed explanation appears in the main text.

6. Summary and conclusions

Small hydroelectric plants are an under-utilized but viable, clean and cost-effective alternative to large dam facilities. The vast majority of small hydroelectric stations in the world are so called run-of-the-river (RoR) plants. These plants use a channel or penstock to divert water from a flowing river to a turbine and electric generator and can be installed at existing dams, as independent generating facilities, or in private systems that power small communities. This is a key reason why RoR hydroelectric plants are often referred to as environmentally friendly, or green power. What is more, RoR plants offer the possibility of decentralized electrification at relatively low operational and maintenance costs, and their construction is shorter and less complex requiring an overall lower capital investment than their dammed based counterparts. Yet, their lack of a major reservoir has an important drawback, and that is, that their power production is not constant but dependent on natural variations in river discharge. Electricity production may even cease when the discharge drops below the minimum technical inflow of the turbines.

In this paper, we have discussed and/or reviewed the basic elements of a general-purpose numerical model of a RoR plant. This model, called HYPER, is coded in MATLAB and simulates the technical performance, energy production, operational and maintenance costs, and economic profit of a RoR plant in response to a record of river discharge values, and suite of design and construction parameters.

Unlike other modeling approaches developed in hydropower literature, HYPER takes into explicit consideration the design flow, penstock diameter, penstock thickness, specific speed, rotational speed, cavitation, and suction head in evaluating the technical performance, production, cost, and profit of a RoR plant.

A built-in evolutionary algorithm enables the user to maximize automatically the RoR plant's performance by optimizing (among others) turbine type (Kaplan, Francis, Pelton and Crossflow), design flow, quantity (1 or 2), and configuration (serial or parallel), and the penstock diameter. This optimization carefully evaluates each turbine's specific speed and admissible suction head, and returns to the user a Table with calibrated parameter values, energy produced, and total cost, of all four turbines individually and all their parallel configurations, respectively. A graphical user interface (GUI) simplifies HYPER model initialization, setup, simulation and optimization. This interface makes it easy for the user to specify values of all variables, select with a simple mouse-click those design and construction variables that warrant optimization, overwrite, possibly, via upload of text files, the default turbine efficiency curves, and upload the river's flow duration curve. What is more, the GUI also enables the user to select which performance criterion of the plant should be maximized (or minimized, if appropriate) during the optimization. Options include the net present value, total power production, internal rate of return and pay-back time of the plant.

Two case studies with differing site characteristics (head) and flow duration curves (FDCs) were used to illustrate the implementation and numerical results of HYPER. These results confirm earlier literature findings that

1 The optimum size (design flow) and design of a RoR plant (type of turbine(s) and diameter of the penstock) balances energy production with construction and maintenance costs. This requires nonlinear optimization of the design and, possibly, operation variables for a given record of discharge data, followed by a cost-benefit analysis of the plant's expenditures, net economic profit and power production (Lopes de Almeida et al., 2006; Anagnostopoulos and Papantonis, 2007; Papantonis and Andriotis, 1993; Haddad et al., 2011; Mishra et al., 2011; Baños et al., 2011; Basso and Botter, 2012).
2 A single turbine is unable to maximize energy retrieval from the

flowing water in the presence of a large dynamic variations in rive discharge. However, the use of two parallel turbines increases considerably the range of workable flows, and thus effectiveness and flexibility of operation of a RoR plant (Anagnostopoulos and Papantonis, 2007).

3 A hydropower system with two turbines (of different size and/or type) configured in parallel enhances significantly energy production, but at the expense of larger investment and maintenance costs. However, in the presence of large dynamic variations in river discharge, the incremental income generated by the use of two parallel turbines out weights the installation and maintenance costs of the second turbine.

The size and design of a RoR plant are hence key variables that determine in large part the power production. More guidance is needed to delineate more exactly between small and large streamflows. This depends, of course, on site characteristics as well.

Future work will include coupling HYPER with AMALGAM to investigate multi-criteria trade-offs among the design parameters. This will help decision makers determine which design and RoR plant operation is most robust and reliable for given site conditions and river stream characteristics. We will also further refine the GUI so that users can (a) control the integration time step of HYPER to match the resolution of the available input data, (b) upload directly the FDC, or work instead, with a record of discharge values. Lastly, the current version of HYPER does not exhibit a storage capacity. The inflow to the turbine system is simply equivalent to the water flux diverted from the river stream. This resemblances the vast majority of RoR plants. To generalize the applicability of HYPER to RoR plants with a small dam or weir we will add a storage module to the program. This will help satisfy base load demands during wet seasons and manage peak load demands during dry seasons. The use of such module (storage capacity) will have important consequences. Water storage may not only alter the river's flow regime, and, thus affect the operation of downstream RoR hydropower plants, but also impact the robustness and stability of HYPER's fixed step numerical solution. To combat these two issues, we would need to optimize simultaneously the design and/or operation of upstream and downstream RoR plants, and replace Euler's method with a mass-conserving, time variable, integration method to simulate accurately reservoir storage. This latter change would enable HYPER to simulate RoR and dam-based hydropower plants.

7. Software availability

The HYPER model described herein has been developed for MATLAB 7.10.0.499 (R2010a).The HYPER model and its extension $\text{HYPER}_{\text{ION}}$ are available upon request from the authors (vyildiz@uci.edu/jasper@uci.edu). The current source code works as well for more recent MATLAB releases. Those that do not have access to MATLAB, can use GNU Octave instead. This is a high-level interpreted language as well, and intended primarily for numerical computations. The Octave language is quite similar to MATLAB so that most programs are easily portable. GNU Octave is open-source and can be downloaded for free from the following link: http://www.gnu.org/software/octave/. The GUI is part of the model toolbox, and computation is easily initiated in MATLAB via the command prompt.

Acknowledgments

We greatly appreciate the comments of three anonymous referees that have improved the current version of this manuscript. The first author gratefully acknowledges support from the General Directorate of State Hydraulic Works (DSI-TURKEY).

Nomenclature

P (MW)	Installed capacity
G (m/s^2)	Gravitational acceleration
η_g (−)	Generator efficiency
H_{net} (m)	Net head
H_d (m)	Design head
f (−)	Friction factor
D (m)	Penstock diameter
H_g (m)	Gross head
P_{atm} (Pa)	Atmospheric pressure
H_f (m)	Friction losses
k (m)	Penstock thickness
z_{power} (m)	Altitude of power house above sea level
q_{md} (m^3/s)	Minimum environmental flow
q_{min} (m^3/s)	Minimum turbine flow
z_{tail} (m)	Water elevation at tail race
f_e (Hz)	Electric system frequency
ω (rpm)	Rotational speed of turbine
E_a (kWh)	Annual energy production
E (kWh)	Daily energy production
A_p (m^2)	Cross-sectional area of penstock
$\bar{R}_a$ ($)	Annual average revenue
C_p ($)	Penstock cost
V_{out} (m/s)	Average flow velocity at outlet
N (−)	Population size
d (−)	Search space dimensionality
C_{em} ($)	Cost of electromechanical equipment
a, b, c (−)	Electromechanical cost coefficients
C_{om} (−)	Annual cost of O&M
β (−)	O&M cost coefficient
C_{cw} ($)	Cost of civil works
δ_{jet} (m)	Height of runner above the tailrace
ρ_w (kg/m^3)	Density of water
η (−)	Turbine efficiency
q (m^3/s)	Processed flow rate
O_d (m^3/s)	Turbine design flow
τ (−)	Crossover value
L (m)	Penstock length
V (m/s)	Design flow velocity
ω_s (−)	Specific speed of turbine
H_s (m)	Suction head
H_o (m)	Singular losses
z_{up} (m)	Upstream water elevation
P_v (Pa)	Water vapor pressure
d_s (ton/m^3)	Density of steel
q_{max} (m^3/s)	Maximum turbine flow
$\mathbf{q}_r$ (m^3/s)	n-vector of river discharges
p (−)	Number of poles
P_0 (Pa)	Atmospheric pressure at sea level
r (%)	Annual interest rate
t (days)	Time
$\bar{E}_a$ (kWh)	Annual average power production
T (−)	Number of turbines
R_a ($)	Annual revenue
e_p (¢/kWh)	Energy price
J (−)	Number of generations
λ_{DE} (−)	Algorithmic variable
C_{rf} (−)	Capital recovery factor
L_s (year)	Lifetime of investment
c_{ton} ($/ton)	Penstock cost per ton weight
α (−)	Total cost coefficient
C_t ($)	Total investment cost
ξ (−)	Exchange rate of EUR to USD

References

Abbasi, T., Abbasi, S.A., 2011. Small hydro and the environmental implications of its extensive utilization. Renew. Sustain. Energy Rev. 15 (4), 2134–2143.

Adamkowski, A., Janicki, W., Kubiak, J., Urquiza, G., Sierra, F., Fernández D, J.M., 2006. Water turbine efficiency measurements using the gibson method based on special instrumentation installed inside pipelines. In: 6th International Conference on Innovation in Hydraulic Efficiency Measurements, Portland, Oregon, USA, pp. 1–12.

Aggidis, G.A., Luchinskaya, E., Rothschild, R., Howard, D.C., 2010. The costs of small-scale hydro power production: impact on the development of existing potential. Renew. Energy 35, 2632–2638.

Akinori, F., Watanabe, S., Matsushita, D., Okuma, K., 2010. Development of ducted Darrieus turbine for low head hydropower utilization. Curr. Appl. Phys. 10, S128–S132.

Al-Zubaidy, S., Right, A., 1997. Performance investigation of a hydroelectric power station at Batang Ai-Sarawak. Int. J. Energy Res. 21, 1405–1412.

Alexander, K.V., Giddens, E.P., Fuller, A.M., 2009. Radial- and mixed-flow turbines for low head microhydro systems. Renew. Energy 34, 1885–1894.

Anagnostopoulos, J.S., Dimitris, E.P., 2012. A fast Lagrangian simulation method for flow analysis and runner design in Pelton turbines. J. Hydrodyn. 24 (6), 930–941.

Anagnostopoulos, J.S., Papantonis, D.E., 2007. Optimal sizing of a run-of-river small hydropower plant. Energy Convers. Manag. 48, 2663–2670.

Aslan, Y., Arslan, O., Yasar, C., 2008. A sensitivity analysis for the design of small-scale hydropower plant: kayabogazi case study. Renew. Energy 33, 791–801.

Baños, R., Manzano-Agugliaro, F., Montoya, F.G., Gil, C., Alcayde, A., Gómez, J., 2011. Optimization methods applied to renewable and sustainable energy: a review. Renew. Sustain. Energy Rev. 15 (4), 1753–1766.

Basso, S., Botter, G., 2012. Streamflow variability and optimal capacity of run-of-river hydropower plants. Water Resour. Res. 48.

Berga, L., 2016. The role of hydropower in climate change mitigation and adaptation: a review. Engineering 2 (3), 313–318.

Borges, C.L.T., Pinto, R.J., 2008. Small hydro power plants energy availability modeling for generation reliability evaluation. IEEE Trans. Power Syst. 23 (3), 1125–1135.

Bozorgi, A., Javidpour, E., Riasi, A., Nourbakhsh, A., 2013. Numerical and experimental study of using axial pump as turbine in pico-hydropower plants. Renew. Energy 53, 258–264.

Brealey, R.A., Myers, S.C., 2002. Principle of Corporate Finance, seventh ed. (New York).

Cobb, B.R., Sharp, K.V., 2013. Impulse (Turgo and Pelton) turbine performance characteristics and their impact on pico-hydro installations. Renew. Energy 50, 959–964.

Degirmenci, 2010. Planning of Water and Soil Resources: Principles, Criteria and Examples, third ed. Poyraz Ofset, Ankara (In Turkish).

Delucchi, M.A., Jacobson, M.Z., 2011. Providing all global energy with wind, water, and solar power, Part II: reliability, system and transmission costs, and policies. Energy Pol. 39 (3), 1170–1190.

Demarty, M., Bastien, J., 2011. GHG emissions from hydroelectric reservoirs in tropical and equatorial regions: review of 20 years of CH4 emission measurements. Energy Pol. 39, 4197–4206.

Deppo, L.D., Datei, C., Fiorotto, V., Rinaldo, A., 1984. Capacity and type of units for small run-of-river plants. Journal of International Water Power & Dam Construction 36, 31–47.

Derakhshan, S., Nourbakhs, A., 2008. Experimental study of characteristic curves of centrifugal pumps working as turbines in different specific speeds. Exp. Therm. Fluid Sci. 32, 800–807.

Desai, V.R., Aziz, N.M., 1994. An experimental investigation of cross-flow turbine efficiency. J. Fluid Eng. 116 (3), 545–550.

Douglas, T., 2007. Green Hydro Power: Understanding Impacts, Approvals, and Sustainability of Run-of River Independent Power Projects in British Columbia. Watershed Watch.

Dursun, B., Gokcol, C., 2011. The role of hydroelectric power and contribution of small hydropower plants for sustainable development in Turkey. Renew. Energy 36 (4), 1227–1235.

Egré, D., Milewski, J.C., 2002. The diversity of hydropower projects. Energy Pol. 30, 1225–1230.

Elbatran, A.H., Yaakob, O.B., Ahmed, Y.M., Shabara, H.M., 2015. Operation, performance and economic analysis of low head micro-hydropower turbines for rural and remote areas: a review. Renew. Sustain. Energy Rev. 43, 40–50.

Electricity Market Law. T.R. Official Gazette Law No.6446.

Fahlbuch, F., 1983. Optimum capacity of a run-of-river plant. Journal of International Water Power & Dam Construction 35, 25–37.

Fahlbuch, F., 1986. Optimum capacity and tunnel diameter of run-of-river plants. Journal of International Water Power & Dam Construction 38, 42–55.

Finardi, E.C., Silva, E.L., Sagastizabal, C., 2005. Solving the unit commitment problem of hydropower plants via Lagrangian Relaxation and Sequential Quadratic Programming. Comput. Appl. Math. 24 (3), 317–341.

Fleten, S.E., Kristoffersen, T.K., 2008. Short-term hydropower production planning by stochastic programming. Comput. Oper. Res. 35 (8), 2656–2671.

Gibson, N.R., 1923. The Gibson Method and Apparatus for Measuring the Flow of Water in Closed Conduits. ASME Power Division, pp. 343–392.

Gingold, P.R., 1981. The optimum size of small run-of-river plants. Journal of International Water Power & Dam Construction 33, 26–39.

Gordon, J.L., Penman, A.C., 1979. Quick estimating techniques for small hydro potential. Int. Water Power Dam Constr. 31, 46–51.

Gorla, L., Perona, P., 2013. On quantifying ecologically sustainable flow releases in a diverted river reach. J. Hydrol. 489, 98–107.

Guide on How to Develop a Small Hydropower Plant. European Small Hydropower Association (ESHA).

Haddad, O.B., Moradi-Jalal, M., Mariño, M.A., 2011. Design operation optimization of run-of-river power plants. Proc. Inst. Civ. Eng. Water Manage. 164, 463–475.

Hamilton, S.H., ElSawah, S., Guillaume, J.H.A., Jakeman, A.J., Pierce, S.A., 2015. Integrated assessment and modelling: overview and synthesis of salient dimensions. Environ. Model. Software 64, 215–229.

Hänggi, P., Weingartner, R., 2012. Variations in discharge volumes for hydropower generation in Switzerland. Water Resour. Manag. 26, 1231–1252.

Heitz, L.F., 1982. Hydrologic Analysis Programs for Programmable Calculators and Digital Computers for Use in Hydropower Studies. University of Idaho Water Resources Research Institute, pp. 127 Report No: 198207.

Heitz, L.F., Khosrowpanah, Sh, 2012. Prediction of Flow Duration Curves for Use in Hydropower Analysis at Ungaged Sites in Kosrae. FSM, University of Guam/WERI Technical, pp. 28 Report No. 137 under printing.

Hobbs, B.F., Mittelstadt, R.L., Lund, J.R., 1996. Energy and water, chapter 31. In: Mays, L.W. (Ed.), Water Resources Handbook, International Edition. McGraw-Hill, New York.

Hosseini, S.M.H., Forouzbakhsh, F., Rahimpoor, M., 2005. Determination of the optimal installation capacity of small hydro-power plants through the use of technical, economic and reliability indices. Energy Pol. 33, 1948–1956.

Hydropower Market Analysis by Application (Industrial, Residential, Commercial) and Segment Forecasts to 2020, Rep. San Francisco: Grand View Research (2014).

IEC, 1991. 41, International Standard: Field Acceptance Tests to Determine the Hydraulic Performance of Hydraulic Turbines, Storage Pumps and Pump-turbines.

Kaldellis, J.K., Vlachou, D.S., Korbakis, G., 2005. Techno-economic evaluation of small hydro power plants in Greece: a complete sensitivity analysis. Energy Pol. 33, 1969–1985.

Karlis, A.D., Papadopoulos, D.P., 2000. A systematic assessment of the technical feasibility and economic viability of small hydroelectric system installations. Renew. Energy 20, 253–262.

Khosrowpanah, S., Fiuzat, A., Albertson, M., 1988. Experimental study of cross flow turbine. J. Hydraul. Eng. 114 (3), 299–314.

Khurana, S., Kumar, V., Kumar, A., 2013. The effect of nozzle angle on erosion and the performance of turgo impulse turbines. Int. J. Hydropower Dams 20, 97–101.

Knight Piesold Consulting, 2008. Plutonic Hydro Inc. Bute Inlet Project. Summary of Project Intake and Turbine Parameters.

Kumar, A., Schei, T., Ahenkorah, A., Caceres Rodriguez, R., Devernay, J.M., Freitas, M., Hall, D., Killingtveit, Å., Liu, Z., 2011. Hydropower. In: Edenhofer, O., Pichs-Madruga, R., Sokona, Y., Seyboth, K., Matschoss, P., Kadner, S., Zwickel, T., Eickemeier, P., Hansen, G., Schlömer, S., von Stechow, C. (Eds.), IPCC Special Report on Renewable Energy Sources and Climate Change Mitigation. Cambridge University Press, Cambridge, United Kingdom and New York.

Lafitte, R., 2014. World Hydro Power Potential. International Sustainable Energy Organization for Renewable Energy and Energy Efficiency Retrieved 8 Dec, 2014, from. http://www.uniseo.org/hydropower.html.

Laghari, J.A., Mokhlis, H., Bakar, A.H.A., Mohammad, H., 2013. A comprehensive overview of new designs in the hydraulic, electrical equipments and controllers of mini hydro power plants making it cost effective technology. Renew. Sustain. Energy Rev. 20, 279–293.

Laniak, G.F., Olchin, G., Goodall, J., Voinov, A., Hill, M., Glynn, P., Whelan, G., Geller, G., Quinn, N., Blind, M., Peckham, S., Reaney, S., Gaber, N., Kennedy, R., Hughes, A., 2013. Integrated environmental modeling: a vision and roadmap for the future. Environ. Model. Software 39, 3–23.

Law on Utilization of Renewable Energy Sources for the Purpose of Generating Electrical Energy. T.R. Official Gazette Law No.5346.

Letcher, R.A., Croke, B.F.W., Merritt, W.S., Jakeman, A.J., 2006. An integrated modelling toolbox for water resources assessment and management in highland catchments: sensitivity analysis and testing. Agric. Syst. 89, 132–164.

Liu, X., 2000. Application of ultrasonic flow measurement technologies on the testing of hydroelectric generating units in China. J Hydro Power Plant Automat supplement edition. https://www.sciencedirect.com/science/article/pii/S0736584515300648 (In Chinese).

Liu, Y., Ye, L., Benoit, I., Liu, X., Cheng, Y., Morel, G., Fu, C., 2003. Economic performance evaluation method for hydroelectric generating units. Energy Convers. Manag. 44, 797–808.

Lopes de Almeida, J.P.P.G., Lejeune, A.G.H., Sá Marques, J.A.A., Cunha, M.C., 2006. OPAH a model for optimal design of multipurpose small hydropower plants. Adv. Eng. Software 37, 236–247.

Maekawa, M., Miyagawa, K., Komuro, T., Fukuda, H., 2003. Study of cavitation erosion on hydraulic turbines runners. In: Fifth International Symposium on Cavitation (CAV2003), Cav03-OS-6-015, pp. 1–7.

Maier, H.R., Kapelan, Z., Kasprzyk, J., Kollat, J., Matott, L.S., Cunha, M.C., Dandy, G.C., Gibbs, M.S., Keedwell, E., Marchi, A., Ostfeld, A., Savic, D., Solomatine, D.P., Vrugt, J.A., Zecchin, A.C., Minsker, B.S., Barbour, E.J., Kuczera, G., Pasha, F., Castelletti, A., Giuliani, M., Reed, P.M., 2014. Evolutionary algorithms and other metaheuristics in water resources: current status, research challenges and future directions. Environ. Model. Software 62, 271–299.

Manuals and Guidelines for Micro-hydropower Development in Rural Electrification, 2009. Department of Energy, Energy Utilization Management Bureau, vol. 1.

Mao, G., Wang, S., Tenq, Q., Zuo, J., Tan, X., Wang, H., Liu, Z., 2017. The sustainable future of hydropower: a critical analysis of cooling units via the Theory of Inventive Problem Solving and Life Cycle Assessment methods. J. Clean. Prod. 142 (4), 2446–2453.

MEA (Millenium Ecosystem Assessment), 2005. Ecosystems and Human Well-being: Synthesis. Island Press.

Mishra, S., Singal, S.K., Khatod, D.K., 2011. Optimal installation of small hydropower

plant—A review. Renew. Sustain. Energy Rev. 15 (8), 3862–3869.
Momoh, J.A., El-Hawary, M.E., Adapa, R., 1999a. A review of selected optimal power flow literature to 1993, part I: nonlinear and quadratic programming approaches. IEEE Transactions on Systems 14 (1), 96–104.
Momoh, J.A., El-Hawary, M.E., Adapa, R., 1999b. A review of selected optimal power flow literature to 1993, part II: Newton, linear programming and interior point methods. IEEE Transactions on Systems 14 (1), 105–111.
Montanari, R., 2003. Criteria for the economic planning of a low power hydroelectric plant. Renew. Energy 28, 2129–2145.
Motwani, K.H., Jain, S.V., Patel, R.N., 2013. Cost analysis of pump as turbine for pico hydropower plants – a case study. Procedia Engineering 51, 721–726.
Najmaii, M., Movaghar, A., 1992. Optimal design of run-of-river power plants. Water Resour. Res. 28, 991–997.
Niadas, I.A., Mentzelopoulos, P., 2008. Probabilistic flow duration curves for small hydro plant design and performance evaluation. Water Resour. Manag. 22, 509–523.
Nicklow, J., Reed, P., Savic, D., Dessalegne, T., Harrell, L., Chan-Hilton, A., Karamouz, M., Minsker, B., Ostfeld, A., Singh, A., Zechman, E., 2010. State of the art for genetic algorithms and beyond in water resources planning and management. J. Water Resour. Plann. Manag. 136 (4), 412–432.
Nouni, M.R., Mullick, S.C., Kandpal, T.C., 2006. Techno-economics of micro-hydro projects for decentralized power supply in India. Energy Pol. 34 (10), 1161–1174.
Ogayar, B., Vidal, P.G., 2009. Cost determination of the electromechanical equipment of a small hydro-power plant. Renew. Energy 34, 6–13.
Okot, D.K., 2013. Review of small hydropower technology. Renew. Sustain. Energy Rev. 26, 515–520.
Olgun, H., 1998. Investigation of the performance of a cross flow turbine. Int. J. Energy Res. 22, 953–964.
Paish, O., 2002a. Small hydro power: technology and current status. Renew. Sustain. Energy Rev. 6, 537–556.
Paish, O., 2002b. Micro-hydro power: status and prospects. Journal of Power and Energy 216, 31–40.
Palmer, M.A., Bernhardt, E.S., Schlesinger, W.H., 2010. Mountaintop mining consequences. Science 327, 148–149.
Pandey, B., Karki, A., 2017. Hydroelectric Energy. Renewable Energy and the Environment CRC Press/Taylor Group.
Papantonis, D.E., Andriotis, G., 1993. Optimization of the size and number of turbines for a small hydropower plant. Proceedings, Hidroenergia 3, 59–68.
Parker, G.J., 1996. A theoretical study of the performance of an axial flow turbine for a micro hydro installation. Proc. Inst. Mech. Eng. Part A: Journal Power Energy 210, 121.
Parker, P., Letcher, R., Jakeman, A., Beck, M.B., Harris, G., Argent, R.M., Hare, M., Pahl-Wostl, C., Voinov, A., Janssen, M., Sullivan, P., Scoccimarro, M., Friend, A., Sonnenshein, M., Barker, D., Matejicek, L., Odulaja, D., Deadman, P., Lim, K., Larocque, G., Tarikhi, P., Fletcher, C., Put, A., Maxwell, T., Charles, A., Breeze, H., Nakatani, N., Mudgal, S., Naito, W., Osidele, O., Eriksson, I., Kautsky, U., Kautsky, E., Naeslund, B., Kumblad, L., Park, R., Maltagliati, S., Girardin, P., Rizzoli, A., Mauriello, D., Hoch, R., Pelletier, D., Reilly, J., Olafsdottir, R., Bin, S., 2002. Progress in Integrated Assessment and Modelling, vol. 17. Environmental Modelling & Software, pp. 209–217.
Peña, R., Medina, A., Anaya-Lara, O., McDonald, J.R., 2009. Capacity estimation of a minihydro plant based on time series forecasting. Renew. Energy 34, 1204–1209.
Penche, C., 1998. Layman's Handbook: on How to Develop a Small Hydro Site, Published by the European Small Hydropower Association (ESHA), second ed. .
Pimnapat, I., Patib, T., Bhumkittipichc, K., 2013. Performance study of micro hydro turbine and PV for electricity generator, case study: bunnasopit School, y Nan province, Thailand, 10th eco-energy and materials science and engineering (EMSES2012). Energy Proc 34, 235–242.
Price, K.V., Storn, R.M., Lampinen, J.A., 2005. Differential Evolution, a Practical Approach to Global Optimization. Springer, Berlin.
Ramos, H., Betâmio De Almeida, A., Manuela Portela, M., Pires De Almeida, H., 2000. Guideline for Design of Small Hydropower Plants.
Ramos, H.M., Simão, M., Borga, A., 2013. Experiments and CFD analyses for a new reaction micro hydro propeller with five blades. J. Energy Eng. 139, 109–117.
Renewable energy technologies: cost analysis series. International Renewable Energy Agency (IRENA) 1 Power Sector.
Sadegh, M., Vrugt, J.A., Gupta, H.V., Xu, C., 2015. The soil water characteristic as new class of closed-form parametric expressions for the flow duration curve. J. Hydrol. 535 (2016), 438–456.
Santolin, A., Cavazzini, G., Pavesi, G., Ardizzon, G., Rossetti, A., 2011. Techno-economical method for the capacity sizing of a small hydropower plant. Energy Convers. Manag. 52, 2533–2541.
Sharma, D.P., Verma, G.L., Bahadur, A.K., 1980. Selecting installed capacity for a run-of-river plant. Journal of International Water Power & Dam Construction 32, 23–26.
Sharma, M.G., Das, D., Sharma, J., 2002. Selection of optimum capacity for run-of-river plant. Journal of Dam Engineering 23, 97–117.
Shimokawa, K., Furukawa, A., Okuma, K., Matsushita, D., Watanabe, S., 2012. Experimental study on simplification of Darrieus-type hydro turbine with inlet nozzle for extra-low head hydropower utilization. Renew. Energy 41, 376–382.
Singal, S.K., Saini, R.P., Raghuvanshi, C.S., 2010. Analysis for cost estimate of low head run-of-river small hydropower schemes. Energy for Sustainable Development 14, 117–126.
Singh, P., Nestmann, F., 2009. Experimental optimization of a free vortex propeller runner for micro-hydro application. Exp. Therm. Fluid Sci. 33, 991–1002.
Small Hydro Project Analysis, 2004. Retscreen Engineering & Cases Textbook. pp. 37–47.
Storn, R., Price, K., 1997. Differential evolution - a simple and efficient heuristic for global optimization over continuous spaces. J. Global Optim. 11, 341–359.
The World Bank, 2017. World Development Indicators. Washington, D.C.
Troskolanski, A., 1960. Hydrometry. Pergamon Press Ltd.
US Energy Information Administration, 2016. Monthly Energy Review, Table 1.3 and 10.1.
US Army Corps of Engineers (USACE), 1985. Hydropower Engineering and Design, Engineering Manual 1110-2-1701. US Army Corps of Engineers, Washington, DC.
Vogel, R.M., Fennessey, N.M., 1995. Flow duration curves II: a review of applications in water resources planning. J. Am. Water Resour. Assoc. 31 (1995), 1029–1039.
Voros, N.G., Kiranoudis, C.T., Maroulis, Z.B., 2000. Short-cut design of small hydroelectric plants. Renew. Energy 19, 545–563.
Vrugt, J.A., Robinson, B.A., 2007. Improved evolutionary optimization from genetically adaptive multimethod search. Proc. Natl. Acad. Sci. U.S.A. 104, 708–711.
Vrugt, J.A., ter Braak, C.J.F., Clark, M.P., Hyman, J.M., Robinson, B.A., 2008. Treatment of input uncertainty in hydrologic modeling: doing hydrology backward with Markov chain Monte Carlo simulation. Water Resour. Res. 44.
Vrugt, J.A., ter Braak, C.J.F., Diks, C.G.H., Higdon, D., Robinson, B.A., Hyman, J.M., 2009. Accelerating Markov chain Monte Carlo simulation by differential evolution with self-adaptive randomized subspace sampling. Int. J. Nonlinear Sci. Numer. Stimul. 10 (3), 273–290.
Wallace, A.R., Whittington, H.W., 2008. Performance prediction of standardized impulse turbines for micro-hydro, *Sutton*. Int. Water Power Dam Constr Elsevier B.V., U.K, https://www.sciencedirect.com/science/article/pii/S1364032114009769.
Williams, A.A., 1994. The turbine performance of centrifugal pumps: a comparison of prediction methods. Proc. Inst. Mech. Eng. Part A: Journal Power Energy 208, 59.
Williamson, S.J., Stark, B.H., Booker, J.D., 2013. Performance of a low-head pico-hydro turgo turbine. Appl. Energy 102, 1114–1126.
Williamson, S.J., Stark, B.H., Booker, J.D., 2014. Low head pico hydro turbine selection using a multi-criteria analysis. Renew. Energy 61, 43–50.
wivedi, D., Raja, A.K., 2006. Amit Prakash Srivastava, Manish, Power Plant Engineering. New Age International, New Delhi, pp. 354.
World Atlas, Industry Guide, 2010. International Journal of Hydropower and Dams.
Yaakob, O.B., Ahmed, Y.M., Elbatran, A.H., Shabara, H.M., 2014. A review on micro hydro gravitational vortex power and turbine systems. Jurnal Teknologi (Sci Eng) 69 (7), 1–7.
Yassi, Y., Hashemloo, S., 2010. Improvement of the efficiency of the agnew micro-hydro turbine at part loads due to installing guide vanes mechanism. Energy Convers. Manag. 51, 1970–1975.
Ye, L., Weidong, L., Zhaohui, L., Malik, O.P., Hope, G.S., 1995. An integral criterion appraising the overall quality of a computer-based hydro turbine generating system. IEEE Trans. Energy Convers. 10 (2), 376–381.
Ye, L., Li, Z., Liu, Y., Zhang, Y., 2000. Intelligent Control-maintenance-management System and its Applications on Hydropower System. Management and Control of Production and Logistics 2000, vol. 2. IFAC/IFIP/IEEE, Pergamon, pp. 609–614.
Ye-xiang, X., Feng-qin, H., Jing-lin, Z., Takashi, K., 2007. Numerical prediction of dynamic performance of Pelton turbine. Journal of Hydrodynamics, Ser. B 19 (3), 356–364.
Yoo, J.H., 2009. Maximization of hydropower generation through the application of a linear programming model. J. Hydrol. 376 (1–2), 182–187.
Zheng, Q., 1997. Test of turbine efficiency and economic benefit. Yunnan Water Power 47 (2), 91–96 (In Chinese).